

# Augmentation of Muscular Endurance in Lower-Limb Exercises via a Passive Elastic Exoskeleton.

by

Nicolas Hite

A senior design project submitted in partial fulfillment of the requirements for the degree of Bachelor of Science in Engineering Sciences at Harvard University

S.B. Degree Candidate in Engineering Sciences

MIT Advisor: Elliott Rouse  
SEAS Advisor: Katia Bertoldi

Harvard University School of Engineering and Applied Sciences  
Cambridge, MA

April 21, 2014

## Abstract

The research and production of exoskeleton devices has resulted in many amazing products for application in the military and rehabilitative use for the physically disabled. However, these products are often bulky, heavy, complex, and expensive due to the actuators and power supplies required to operate them. The Biomechatronics group at the MIT Media Lab has conducted experiments proving that muscular endurance can be augmented significantly using a simple system of passively powered springs; this finding has opened the door to widespread application of passive exoskeleton device that are simple, lightweight, compact, and feasible for use in everyday labor-intensive tasks or even recreation.

This project aims to extend the results of the Biomechatronics group using a set of flexible fiberglass leaf springs to increase muscular endurance in the lower limbs during exercises like squatting and lower-limb-powered lifting. Such progress aims to pave the way toward making exoskeleton devices available to the common individual, such as manual labourers who squat several times throughout their workday. The exoskeleton springs were constructed and characterized to provide substantial upward force for a load of around 250 lbs. Characterization was completed using computer vision analysis of the springs' deformation under various loading cycles. The efficacy of the device was tested on several subjects while measuring changes in metabolic data such as oxygen consumption and specific power exertion. The exoskeleton was found to have a substantial effect on lowering the metabolic needs of an individual during repetitive squatting.

# CONTENTS

<b>I</b>	<b>Introduction</b>	7
I-A	Motivation . . . . .	7
I-B	Literature Review: State of the Art and Patent Search . . . . .	8
I-C	Potential Users . . . . .	12
<b>II</b>	<b>Design Goals</b>	14
<b>III</b>	<b>Design Approach</b>	17
III-A	Ideation . . . . .	17
III-B	Feasibility Consideration of the TSSLs . . . . .	18
<b>IV</b>	<b>Design Details</b>	20
IV-A	Known Factors . . . . .	20
IV-B	Unknown Factors . . . . .	22
IV-C	Standards . . . . .	23
<b>V</b>	<b>Prototyping Narrative</b>	24
V-A	Design Evolution . . . . .	24
V-A1	Leaf Springs . . . . .	24
V-A2	Thigh Connection . . . . .	26
V-A3	Boot Connection . . . . .	28
V-A4	Hinges . . . . .	29
V-A5	Combining . . . . .	30
V-B	Fabrication and Redesign . . . . .	31
V-B1	Leaf Springs . . . . .	31
V-B2	Thigh Connection . . . . .	33
V-B3	Boot Connection . . . . .	33
V-B4	Hinges . . . . .	34
V-B5	Combining . . . . .	34
<b>VI</b>	<b>Spring Characterization</b>	35
VI-A	Experimental Design . . . . .	35
VI-B	Least-Squares Analysis of Stiffness Matrices . . . . .	36
<b>VII</b>	<b>Exoskeleton Testing on Metabolic Data</b>	39
VII-A	Experimental Design . . . . .	39
VII-B	Shifting the Coordinate System . . . . .	40
VII-C	Stiffness Extrapolation . . . . .	41
VII-D	Calculating Force . . . . .	42
VII-E	Calculating Energy Storage and Release . . . . .	42
<b>VIII</b>	<b>Results</b>	44
VIII-A	Stiffness Characterization Data . . . . .	44
VIII-B	Metabolic Advantage . . . . .	47
VIII-C	Calculating Squat Test Force . . . . .	48
VIII-D	Energy Storage, Release, and Damping . . . . .	50
<b>IX</b>	<b>Budget</b>	52

<b>X</b>	<b>Conclusion</b>	53
X-A	Significance . . . . .	53
X-B	Future Work . . . . .	53
X-C	Context . . . . .	54
<b>XI</b>	<b>Acknowledgements</b>	55
<b>References</b>		56
<b>Appendix A: Bill of Materials</b>		57
<b>Appendix B: Design Drawings</b>		58
<b>Appendix C: MATLAB Code</b>		74
C-A	Exo Video Processing . . . . .	74
C-B	Stiffness Matrix Calculations . . . . .	78

# LIST OF FIGURES

1	A comparison of lifting techniques: squatting (right) versus stooping (left). (image source: www.mastergarden products.com/gardenerscorner/kneesback.htm)	7
2	Early designs and prototypes for exoskeleton devices. From left to right: Yagn's assistive running device, the Hardiman from GE, and the BLEEX device (image credit Prof. Homayoon Kazerooni).	8
3	EHPA-stimulated exoskeleton projects. From left to right: MIT quasi-passive exoskeleton, the HAL-5, the Nurse- Assisting Exoskeleton, the RoboKnee. Image credits: Hugh Herr, Biomechatronics Laboratory, MIT Media Lab; Prof. Sankai, University of Tsukuba/CYBERDYNE, Inc.; Prof. Keijiro Yamamoto, Kanagawa Institute of Technology.	9
4	A patient with neuromuscular weakness uses a passive WREX orthosis. Image credit Wilmington Robostics.	10
5	Part (a) depicts the configuration of wrist-waist springs set up for muscular endurance testing. (b) shows the results of normalized cycles until exhaustion (y axis) versus the spring constant of the wrist-waist springs (x axis). Image credit: Hugh Herr, Biomechatronics group, MIT Media Lab, Cambridge, MA.	10
6	Diagram of the passive exoskeleton device.	11
7	Diagram of the lower-limb exoskeleton.	11
8	Diagram of the skiing exoskeleton.	12
9	Visualization of the gait cycle. We can see that the knee stays at relatively small angles during the stance phase with the body weight on the leg. During the swing phase, the knee swings to $\sim 45^\circ$ , and since there is no load, the only contributing factor to torque are the muscles in the leg	15
10	The angles of the three main joints in the leg over a single gait cycle. The knee, the critical joint here, is highlighted in red. The maximum value, once again is $\sim 45^\circ$ .	15
11	A quick sketch of how the Thigh-Shank Single Leaf Spring would look and function.	17
12	A close-up view of the SolidWorks model for the thigh connection of the TSSLS solution. Note how the free rotation of the spring can be engaged and disengaged by the dogtooth-clutch system, which is controlled by the lever arm.	18
13	A general view of the TSSLS SolidWorks model.	18
14	A visualization of how the proposed passive elastic exoskeleton will work. The spring force increases along with the extent of the user's squat motion—at the lowest point, it provides the most upward force.	20
15	s-n curve: a look at the fatigue lifespans of multiple types of fiberglass. Since the leaf springs will be bending, the stresses of import are the flexural loads, as represented by the dashed lines. All nonwoven, unidirectional fiberglass has a high fatigue lifespan (Source: ASM Engineer's Guide to Composite Materials).	21
16	(a) SolidWorks model of the TSMLS spring. (b) Intended orientation with user's leg.	24
17	The thigh connection to the spring.	26
18	The combat boot.	28
19	Finite Element Analysis of the strap hinge.	29
20	The completed design of the exoskeleton.	30
21	A view of each leaf spring before assembly.	31
22	A view of the spring after assembly.	31
23	Trouble with flange attachments.(a) Upon epoxying, (b) upon failure.	31
24	New flange attachments: (a) SolidWorks model of the new flange piece, (b) flat profile before band saw and bending, (c) the shaped flange before hole addition.	32
25	The thigh connection, attached to the spring. The hinge is visible on the back.	33
26	The boot connection to the spring.	33
27	How to wear the exoskeleton.	34
28	The force sensor.	35
29	The spring, clamped in the vise.	36
30	A visualization of MATLAB's point-tracking algorithm. The two tracked points are the two endpoints of the red vector, which defines the angle of applied force.	37
31	A visualization of the least-squares analysis.	37

32	(a) Metabolic testing. (b) Setup of the COSMED system for metabolic data acquisition. . . . .	39
33	Shifting the coordinate system. The two green lines indicate the distance from boot to thigh connection—the line terminating with the red '+' sign is unshifted. Blue '+' is shifted. The line in the lower right tracks the angle of the boot hinge. . . . .	41
34	Comparing squat-test deformations (red) to characterization deformations (black). Though the ranges and paths traveled by the spring are close, they are not an exact match. . . . .	41
35	The force and deformation data for both tests. . . . .	44
36	The locations of negative principle stiffnesses in trial 2. . . . .	45
37	Formation of an ellipse through eigenvectors. . . . .	46
38	Visualization of stiffness via eigen-ellipses. Here, the green vector represents the applied force, and the cyan and red vectors (scaled) represent the principle and off-axis stiffnesses. . . . .	46
39	Metabolic data by COSMED. The bolded segment is the window chosen to compute specific power consumption. . . . .	47
40	The force and deformation profiles of the squat test. These have been rotated, extrapolated, integrated, and re-rotated from the squat deformation data. . . . .	48
41	Ellipse visualizations of the squat tests. The force is represented by the green vector, and the red ellipse is defined by the eigenvalues and eigenvectors of the stiffness matrices. . . . .	49
42	The energy storage and release of the TSMLS spring. . . . .	50

## LIST OF TABLES

I	A summary of desired design specifications. . . . .	16
II	The revisited design decision matrix. Taking this new factor into account, the TSMLS emerges at the best solution. . . . .	19
III	A summary of spring dimensions. . . . .	25
IV	Comparison of fatigue tolerances in 1/8" thick and 1/5" thick fiberglass. . . . .	26
V	A summary of thigh connection dimensions. . . . .	27
VI	A summary of boot connection dimensions. . . . .	28
VII	The accuracy of stiffness matrix estimation. . . . .	45
VIII	The accuracy of stiffness matrix estimation. . . . .	47
IX	Squat test calculated forces and deformations. . . . .	48
X	Squat test calculated forces and deformations. . . . .	50
XI	A summary of desired design specifications. . . . .	53

# I. INTRODUCTION

## A. Motivation

The attention to the form and technique of the practice of manual-labor style lifting in the workplace receives relatively little attention compared to the substantial effect it has on the health of workers around the world. The U.S. Bureau of Labor Statistics has declared that more than one million workers suffer back injuries each year, and back injuries account for one of every five workplace injuries or illnesses [1]. Of these injuries, about 80% are to the lower back, and 75% of them occur during lifting [2].

While it has been proposed that an ergonomic makeover of such workplace tasks be considered as the most effective long-term solution, other engineering solutions can be found while analyzing lifting technique. A noticeable factor in lower back injuries is poor lifting technique—users that tend to *stoop*, or bend forward at the waist or mid-back to lift objects are correlated with a much higher risk of low back disorders (LBDs) than users who *squat*, or bend at the knees so that the buttocks rest on or near the heels [3]. This is due to high spinal compression caused by the stooping posture as well as shear stresses associated with repeated spinal flexion [3], [4]. Proper lifting technique utilizes a squatting motion that eases the stresses on the back relative to the stoop, but workers often resort to stooping because it is less fatiguing and demands less leg strength and endurance [3].

In an effort to simultaneously encourage proper lifting technique and reduce energy expenditure to augment muscular endurance, we propose a lower-limb exoskeleton device that stores energy from a squat-like motion in a set of leaf springs, which provide an upward force and assist the user with their task.



Fig. 1: A comparison of lifting techniques: squatting (right) versus stooping (left). (image source: [www.mastergardenproducts.com/gardenerscorner/kneesback.htm](http://www.mastergardenproducts.com/gardenerscorner/kneesback.htm))

## B. Literature Review: State of the Art and Patent Search

The notion of using an exoskeleton device—that is, an artificial external full or partial skeleton to protect the body or aid in biomechanical functions such as walking, running, climbing, carrying weight, and limb movement—has existed for at least a century [5]. Science-fiction-like ideas to push the limits of human ability were proposed in the realms of both amplifying able-bodied humans and orthopedics, assisting physically impaired individuals via external devices [5]. The first recorded evidence of a proposed exoskeleton device is a set of U.S. Patents given to Nicholas Yagn in 1890 for a device proposed to passively assist in running and jumping via a system of springs; however, there is no evidence that any prototypes were ever created or tested [6].

It is only in the last few decades that technology has advanced to the level at which fabrication of such devices can be seriously researched and prototyped, and more prolific research of exoskeleton devices began in the 1960s. This was mainly by the U.S. Army and Navy in cooperation with major technology companies like General Electric to develop more complex, powered exoskeletons that could augment the physical capabilities of soldiers. These ranged from load-bearing orthopedic supplements to giant, hulking machines [7], [8].



Fig. 2: Early designs and prototypes for exoskeleton devices. From left to right: Yagn's assistive running device, the Hardiman from GE, and the BLEEX device (image credit Prof. Homayoon Kazerooni).

Recent efforts to fortify exoskeleton research are due largely to the Exoskeletons for Human Performance Augmentation (EHPA), sponsored by the Defense Advanced Research Projects Agency (DARPA)—this precipitated such ventures as UC Berkeley's Lower Extremity Exoskeleton (BLEEX) [9], which uses its own sensory data to majorly assistive effect in carrying heavy loads as well as its own power supply. Other notable devices include the Wearable Energetically Autonomous Robot (WEAR) from the Sarcos Research Corporation [10], a quasi-passive exoskeleton from the MIT Media Lab's Biomechatronics group [11], the University of Tsukuba's HAL-5 exoskeleton [12], and the Nurse-Assisting Exoskeleton from the Kanagawa Institute of Technology in Japan [13]. All of these lower-limb exoskeleton devices augment human capability for certain tasks even helping nurses transfer patients between stretchers [13].

As shown in Fig. 2., these EHPA-resultant exoskeleton devices have largely gravitated toward large, complex active designs, which also appears to be the trend of most modern exoskeleton research and

prototyping. We must now differentiate between what have been termed active, passive, and quasi-passive types of exoskeleton devices. An active device uses a power supply for its augmentation; a passive device does not. A quasi-passive device, such as the exoskeleton from MIT Media Lab's Biomechatronics group, uses no powered devices to bear load, but utilizes components such as knee-variable dampers [14].

The rise in large active exoskeleton devices has been met with incredibly powerful and durable prototypes—this comes at the cost of a bulky, complex exterior that can draw substantial power, which necessitates a power supply of substantial weight. Though some prototypes such as the Sarcos WEAR model are energetically autonomous, the trade-off between energetic performance and weight is still significant [10]. Other components such as sensors, actuators, and transmissions must be included and calibrated [5]. The necessary bulk, weight, and cost of such complex devices are such that their widespread commercialization and distribution to entities other than the military or wealthy individuals is not feasible with current technologies.



Fig. 3: EHPA-stimulated exoskeleton projects. From left to right: MIT quasi-passive exoskeleton, the HAL-5, the Nurse-Assisting Exoskeleton, the RoboKnee. Image credits: Hugh Herr, Biomechatronics Laboratory, MIT Media Lab; Prof. Sankai, University of Tsukuba/CYBERDYNE, Inc.; Prof. Keijiro Yamamoto, Kanagawa Institute of Technology.

Some other similar devices include the robotic knee explored in *Effects of Robotic Knee Exoskeleton on Human Energy Expenditure*[4]—the robotic knee also uses energy storage to provide upward force to augment muscular endurance during squat-like exercises. However, this device is powered, and our proposal of a passive, human-powered exoskeleton is still unique and unprecedented. Another device mentioned in Herr's and Dollar's state-of-the-art paper is the Roboknee. Detailed in Jerry Pratt et al's *The RoboKnee: An Exoskeleton for Enhancing Strength and Endurance During Walking* [15]. Using series elastic actuators, this provides an additional boost during activities like walking and climbing stairs. Once again, this is different from the thesis device since it is active and not specialized for squatting motions.

Passive exoskeletons and orthoses can be much smaller, simple, and cheap. Passive and quasi-passive exoskeleton devices have seen widespread use as assistive devices for limb movements since the loads and forces being delivered are on the order of fractions of body weight and single limbs, the necessary power delivered can be much smaller [16]. Though active devices still dominate the lower-limb orthosis market as body weight is more significant than that of a single limb, passive devices are ubiquitous in assisting neuromuscular weakness [16].



Fig. 4: A patient with neuromuscular weakness uses a passive WREX orthosis. Image credit Wilmington Robotics.

One project, which this design project aims to extend, stood on the shoulders of these devices and information. Done by the Biomechatronics group at the MIT Media Lab in 1997, this project was a conceptual test that journeyed back toward the use of passive—that is, spring-loaded devices for physical augmentation of an able-bodied individual. During heavy exercise, only a small portion of muscles fatigue [17]. To combat this during a pull-up exercise, a simple set of springs was connected from the wrists to a waist harness by extending the spring during arm extension, energy was stored in the springs that was released when test subject pulled their body up, effectively altering the distribution of fatiguing and nonfatiguing muscles [17]. This alteration was shown to increase efficiency of the exercise and, on average, double muscular endurance over six test subjects. This endurance was calculated using a normalized value of completed pull-up cycles to exhaustion [17].

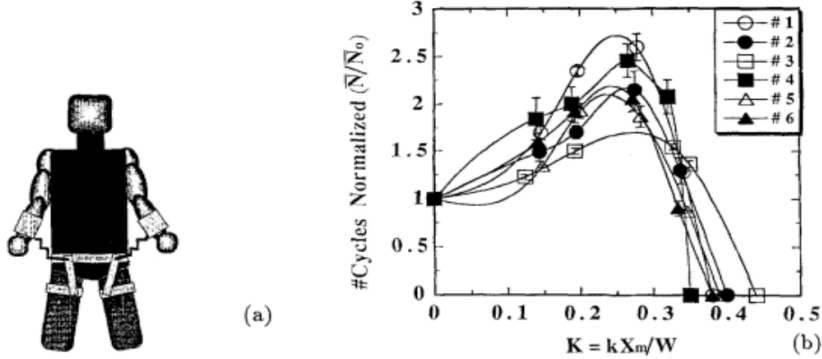


Fig. 5: Part (a) depicts the configuration of wrist-waist springs set up for muscular endurance testing. (b) shows the results of normalized cycles until exhaustion (y axis) versus the spring constant of the wrist-waist springs (x axis). Image credit: Hugh Herr, Biomechatronics group, MIT Media Lab, Cambridge, MA.

This test demonstrated that a real and important quantity such as muscular endurance could be significantly improved by a simple, lightweight passive device, as shown in Fig. 2B, at an optimal spring constant the average increase in muscular endurance was around a factor of two [17]. This technology was extended to a system of energy-storing crutches that boosted the endurance of patients and users via metabolic reduction while climbing stairs [18].

A patent search for similar devices was also conducted. These patents were found on the website uspto.gov.

- 1) **Passive Exoskeleton, Patent No. US 7,571,839 B2**—This device uses a rigid structure and system of sliding rods to transfer some portion of applied loads from the user straight through the ground [19]. Since most load-bearing exoskeleton devices require many actuators, this device is an attempt to circumvent the necessity of such technologies, which may not be invented for a decade or more.

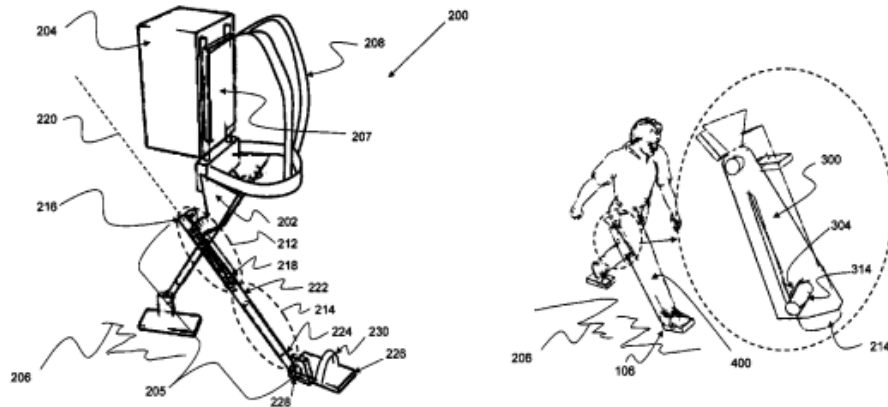
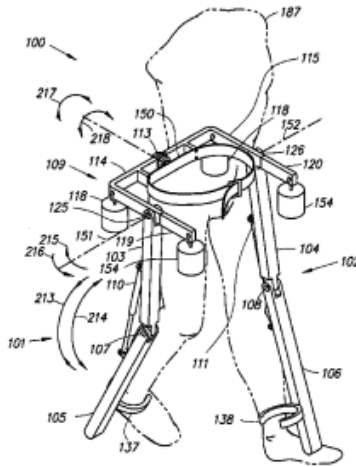


Fig. 6: Diagram of the passive exoskeleton device.

Though this uses nothing but passive components, the device is simply for load bearing during walking and does not provide substantial upward force during a squatting exercise.

- 2) **Lower Extremity Exoskeleton, Patent No. US 7,947,004 B2**—This patented exoskeleton is probably the closest to our proposed device. This consists of thigh and shank links to leg supports that are configured to rest on the ground during normal stance [20]. Using a spring-loaded system comprised of linear compression springs, some flexion and extension of the device is provided by the user.



the lower limbs. However, the patent does not explicitly mention an intended use for the device—it simply lists its claims. Moreover, the device is still heavy and bulky, despite its lack of active components, and it is once again intended for soldiers and not the common manual laborer.

- 3) **Exoskeleton, Patent no. US 8,171,570 B2**—This device is intended not for military or rehabilitative use, but rather for more common recreation. Like our proposed device, it is passive and compact compared to something like the Hardiman or the BLEEX device.

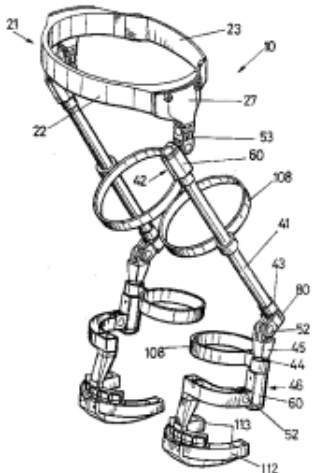


Fig. 8: Diagram of the skiing exoskeleton.

Though this is a passive device, its primary use is to prevent excessive torsion of the knee in recreational activities like skiing. This is primarily a constrictive device to prevent injury and not a way to augment lifting ability [21].

### C. Potential Users

From the literature review it is clear that the popularity of exoskeleton devices has grown exponentially alongside the wealth of new devices being created. As new devices are built, new uses are constantly being considered, but two main needs have become well-cemented: the need for immense power and durability to augment human strength, and the need for responsive devices to assist the physically disabled. Responses to these needs have served to further polarize them in the minds of researchers and developers. Those who design for strength gravitate toward large, complex, and costly powered devices often for military applications, while the more passive ones are geared toward creating assistive and rehabilitative orthoses.

This polarization toward military might and medical assistance limits the potential uses of such devices to carrying extremely heavy loads and helping those who cannot move their own limbs with ease—this fails to capture the middle ground revealed by the Biomechatronics group of the MIT Media Lab. That is, the polarization fails to consider passive exoskeleton devices that can augment the common, able-bodied individual's abilities without that augmentation being necessarily weapons-grade. Consider the needs from recreational climbers already addressed by the Biomech group's simple proof-of-concept experiment: exoskeleton devices can augment human endurance in everyday activities like manual labor

or even recreation. A device need not be able to carry hundreds of pounds of load for it to be useful to the common individual.

As this project aims to construct a lower-limb exoskeleton, consider a manual laborer who picks up boxes or furniture off the ground all day and carry them somewhere else. There are many such jobs in warehouses, factories, moving companies, etc. This is an area where an existing solution, such as a giant, actively powered exoskeleton device is both unwieldy and unnecessary—the worker does not need superhuman strength or to carry the weights several miles, as a soldier might; they simply perform the repetitive task of bend over, lift, place, repeat. Since squat-like motions involve significant leg work, many laborers resort to stooping motions, which can place additional internal moment, compression, and shear stresses on the spine [4]. In such circumstances a simple, passive device that stores the change in gravitational potential energy from the squat could provide a much-needed boost on the return to normal stance. Lifters often wear protective harnesses to keep their backs straight or grip cords attached to the bottoms of heavy objects so they need not crouch as low; however, these solutions, while effective in preventing injury, do not store or utilize the energy that is lost while crouching. Another obvious solution is exercise to gain strength, but an assistive exoskeleton that can provide stored energy should provide benefit at any level of muscular fitness. Machines used to haul objects can not be used in every situation—inevitably, humans must lift.

## II. DESIGN GOALS

The main advantage of this design is that it is simple, compact, lightweight, and much more affordable than other exoskeleton devices. Seeing as it was meant to be applied to the very broad spectrum of manual laborers, the exoskeleton must be able to accommodate a substantial amount of weight. Since the weight of a manual laborer is above average, not to mention that the proposed testers of the device (the author and his advisor) both weigh 180 lbs or more and were over 6'0" in height, *the device should be able to accommodate a user who is 803 N (180 lbf, 81.8 kgf) in weight and 1.83m (6'0") tall or taller.*

If the exoskeleton is to accommodate a user during a squat, then it must be able to bend and deform to the average depth of a manual worker's squat motion. For this reason *the device must be able to accommodate the 90° rotation of the knee and translate downward a distance of around 30 cm without plastic deformation.* The 30 cm value is a measured value of the downward translation of the author's thigh during a typical squat. The user must be able to squat with a knee angle of 90°, with thighs parallel to the ground—this is known as a "parallel squat." Proper lifting technique necessitates a parallel squat because it both maximized dynamic strength and minimizes joint stress [22].

Since weight of the user will vary, it is useful to think of the necessary upward force normalized by weight. In the 1997 Biomechatronics group experiment with passive wrist-waist springs, an optimum F/W (force-weight ratio) was found between 0.2 and 0.3 [8]. It makes sense to set the goal at around this region to start. From there, we can calculate that

$$\text{ratio} \times \text{weight} = \text{upward force}$$

which equates to

$$(0.25)(803N) = 200.75N$$

which means that the device should provide a total upward force of about 200 N.

For the exoskeleton device to be considered a substantial benefit to the user during repetitive squat motions, a large reduction in energy consumption is required. The normalized power consumption of a user is measured in watts per kilogram, and for the device to be considered a success *a metabolic advantage of 10% or greater is required.*

Finally, we must consider the gait cycle when thinking about the exoskeleton. The device must provide substantial upward force at a parallel squat depth without significantly hindering the knees when swinging during normal gait. To understand this a closer look at the gait cycle is required.

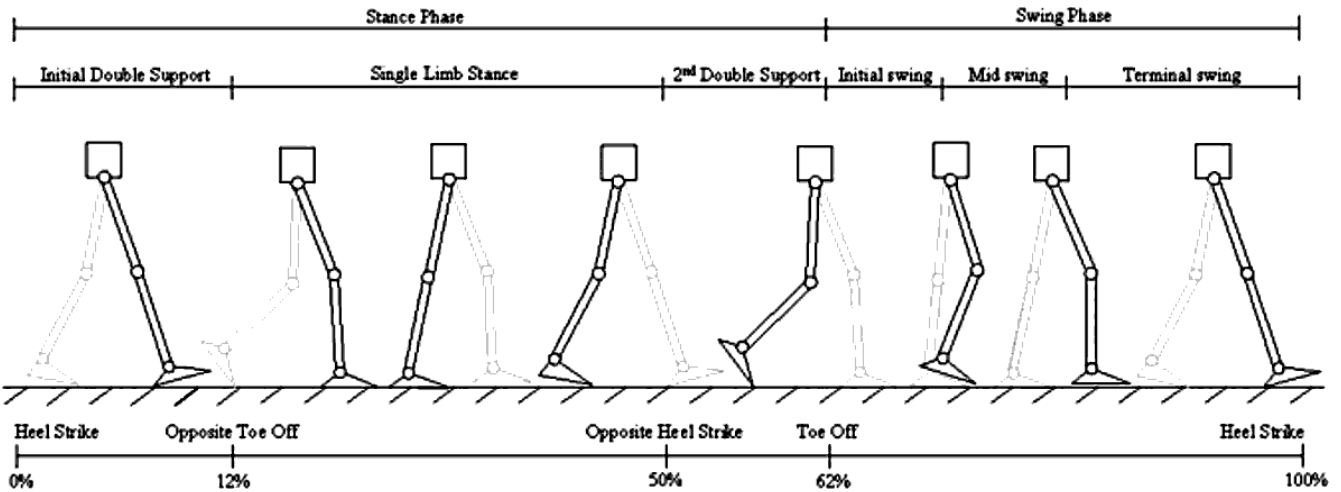


Fig. 9: Visualization of the gait cycle. We can see that the knee stays at relatively small angles during the stance phase with the body weight on the leg. During the swing phase, the knee swings to  $\sim 45^\circ$ , and since there is no load, the only contributing factor to torque are the muscles in the leg

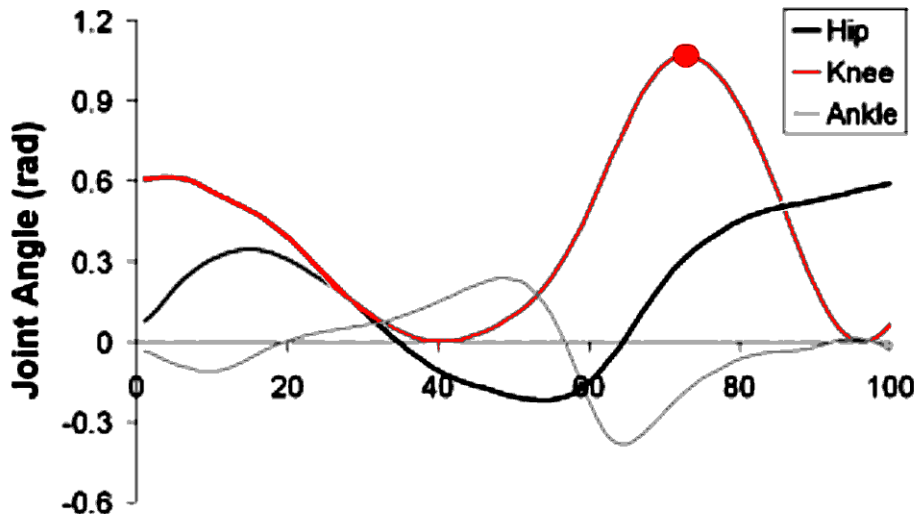


Fig. 10: The angles of the three main joints in the leg over a single gait cycle. The knee, the critical joint here, is highlighted in red. The maximum value, once again is  $\sim 45^\circ$ .

We see that during the normal gait cycle, the knee may bend as much as  $\sim 45^\circ$ . If an exoskeleton device were to be attached, it must be made sure that the device does not provide significant resistive force at this angle. Because the maximum knee angle during gait is about half of a parallel squat, and half of the required 278 N force would still be substantial, a closer look at materials with nonlinear force-deformation characteristics is necessary.

The desired design specifications mentioned are summarized below in Table I.

TABLE I: A summary of desired design specifications.

<b>Design Specification</b>	<b>Desired Value</b>
User Weight	$\sim 800$ N
User Height	$\geq 1.82$ m
Elastic Translation	$\sim 30$ cm
Effective Elastic Rotation	$90^\circ$
Upward Force-Weight Ratio	$\sim 0.25$
Total Upward Force	200 N
Metabolic Advantage	$\geq 10\%$

*Do not interfere substantially with normal gait*

### III. DESIGN APPROACH

#### A. Ideation

We already know that the exoskeleton device must be passive—that is, contain only simple elastic elements, no active or powered components—and that it will use springs. Upon the time of these decisions, however, the exact implementation of the springs—their design and connections to the body—remained ambiguous. The following are the major designs considered for the implementation of the device.

- 1) **Thigh-Shank Single Leaf Spring (TSSLS):** This is a simple implementation that uses a single leaf spring behind each leg. When the user squats, the spring bends along with the legs—the springs' positions behind each leg, not to mention their being parallel to the leg, make this option especially compact. However, due to the geometry of the knee's bending versus the spring's flexing, the spring would have a tendency to push up against the leg. Furthermore, since the distance between the thigh and shank decrease during a squat, there would be significant shear stresses at the connections to the leg. This would require some mechanism that would allow the thigh or shank connection to translate as it was bent, hopefully rolling while also delivering upward force.

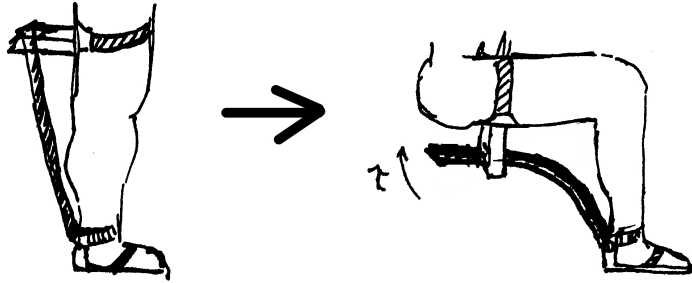


Fig. 11: A quick sketch of how the Thigh-Shank Single Leaf Spring would look and function.

- 2) **Thigh-Shank Multiple Leaf Spring (TSMLS):** Like the Single Leaf Spring implementation, this solution would use springs attached to the back of the thigh and shank; however, the use of multiple leaf springs adds a layer of complexity to the future characterization of spring deformation and stiffness.
- 3) **Thigh-Shank Lateral Leaf Spring (TSLLS):** A different placement of the leaf springs at the lateral ends of the legs would eliminate the problem of the springs pushing up against the legs, as well as the need for a mechanical system allowing the spring connections to translate. However, the torques exerted by the connections would cause the springs to rotate their connection to the front of the leg. Such an instability could be severely hindering.
- 4) **Compression Spring (CS):** This idea briefly returns to helical coil springs as were used in the Biomechatronics Group's 1997 muscular endurance test. Placed on either side of the user and attached at the waist, they would contact the ground directly, eliminating any shear stress on the ankle. The use of coil springs would also make the stiffness of the device easy to characterize. However such a design would be heavier than one using leaf springs, not to mention that the

placement at the sides makes it too bulky to be very maneuverable.

The pros and cons of the potential solutions are explored in greater detail later on—the solutions were judged based on the ability to be compact, lightweight, stable in attachment; as well as having easy characterization and simple connections. The TSSLS was chosen first as a solution to pursue.

## B. Feasibility Consideration of the TSSLS

In order to begin prototyping the Thigh-Shank Single Leaf Spring solution, the first major hurdle had to be overcome: finding a mechanism that will allow the thigh connection of the spring to roll freely—this would prevent the spring from pushing against the back of the user’s legs. If the mechanism could also control the amount of free rotation of the thigh connection, then it would also solve the problem of gait interference during normal walking.

A design was created that incorporated a pair of linear bearings into each spring connection—these would allow the spring to slide up and down the length of the thigh connection. In addition to the translational degree of freedom, a rotational one was added: the rod in between the two linear bearings can rotate freely, meaning the user could walk unhindered while this degree of freedom is engaged. This rotation was controlled by a dogtooth-clutch system, as seen in Fig. 12.

In order for the design to be feasible, the complex motion of the spring under load must be considered—for example, the spring must be able to slide along the thigh connection and provide resistive force simultaneously for the user to get assistance throughout their squat motion. A system that started and stopped providing force suddenly would be startling and unnerving, which could disrupt the normal activity of the user and undermine the efficacy of the solution.

However, a review of the Free-Body Diagram for this solution revealed a fatal error: under load, an unbalanced horizontal force would lead the spring to immediately accelerate the linear bearings along the rod until they hit the hard stops without providing any force—this would mean that for the beginning of the squats, the user would receive no assistance then suddenly feel high resistance. This shock is detrimental to endurance augmentation and necessitates revising and revisiting the other solutions. The decision matrix below (Table II) summarizes the results:

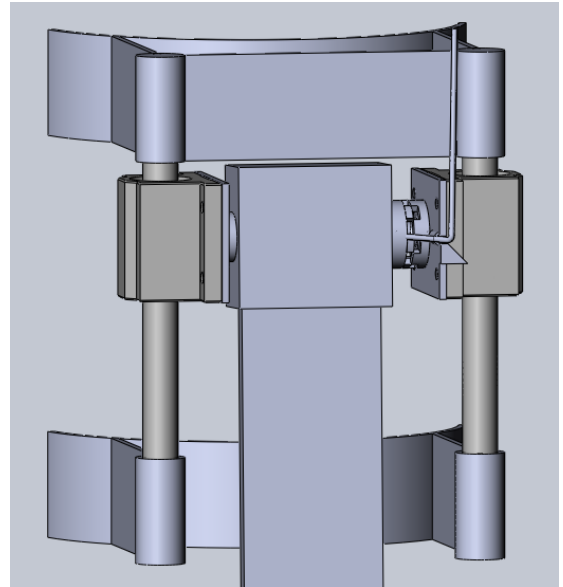


Fig. 12: A close-up view of the SolidWorks model for the thigh connection of the TSSLS solution. Note how the free rotation of the spring can be engaged and disengaged by the dogtooth-clutch system, which is controlled by the lever arm.

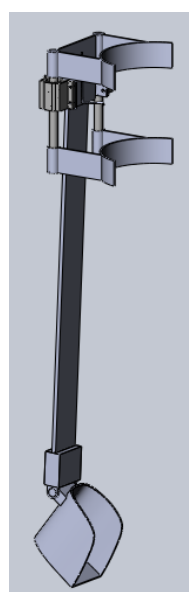


Fig. 13: A general view of the TSSLS SolidWorks model.

TABLE II: The revisited design decision matrix. Taking this new factor into account, the TSMLS emerges at the best solution.

<b>Design Criteria</b>	<b>TSSLS</b>	<b>TSMLS</b>	<b>TSLLS</b>	<b>CS</b>
<b>Compact</b>	++	+	0	-
<b>Lightweight</b>	+	+	+	-
<b>Stable</b>	+	+	-	+
<b>Easy Characterization</b>	+	0	+	+
<b>Simple Connections</b>	-	0	+	+
<b>Smooth Force Profile</b>	-	+	+	+
+	5	4	4	4
0	0	2	1	0
-	2	0	1	2
<b>Total</b>	3	4	3	2

The TSMLS, bending in a C-shaped arc that was the reverse of the TSSLS, would not push against the legs of the user. Thus, no mechanical systems were needed to validation its use, and prototyping could begin.

## IV. DESIGN DETAILS

The passive lower-limb exoskeleton consists of a simple spring-loaded system. When the user crouches down, the springs will flex more, storing the energy from the change in gravitational potential. Upon rising, the springs extend, releasing the energy in the springs as an upward force that assists with lifting. The further the user squats, the more upward force is generated in the springs. It is important to note that the energy for this upward force comes from the drop in gravitational potential energy of the user during squatting—the user need not exert his or her muscles against the spring to bend it. The stiffness of the spring is to be adjusted such that weight alone will be enough to bend the springs to the desired deformation and provide the desired force as outlined in Table I.

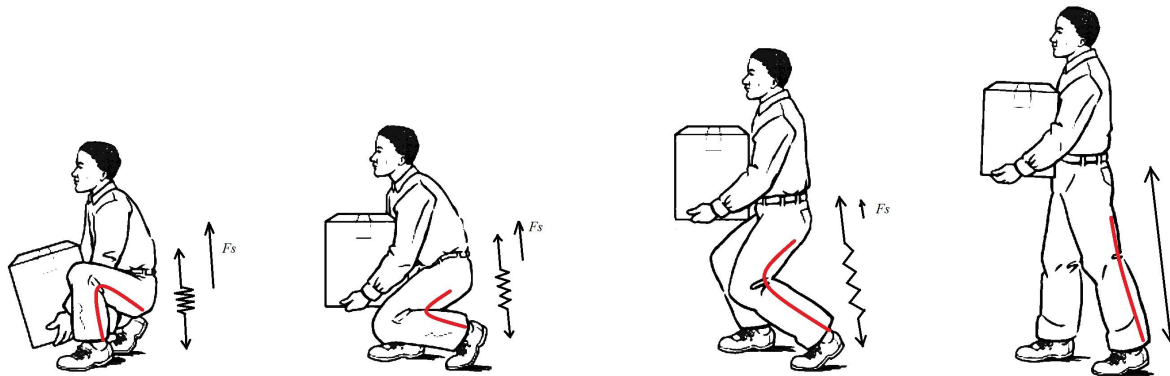


Fig. 14: A visualization of how the proposed passive elastic exoskeleton will work. The spring force increases along with the extent of the user's squat motion—at the lowest point, it provides the most upward force.

Details of the design at this stage could be easily broken down into known and unknown factors.

### A. Known Factors

- 1) **Spring Materials.** After brief consideration, a few different materials were chosen to construct the exoskeleton springs.
  - a) *Fiberglass* for the leaf springs—FRP fiberglass, especially non-woven unidirectional fiberglass (FRP fiberglass that is molded in thermoset plastic and not woven from other sheets into a mat, with all the glass fibers conlinear) is strong and resilient in loading applications. This, as well as its large elastic range of deformation and resistance to fatigue, makes it perfect for cyclical loading, which would occur in repetitive squat motions (see Fig. 15).
  - b) *Aluminum* for any connections and reinforcements between the leaf springs in series. Aluminum is lightweight and easily formable without complex machining being necessary.

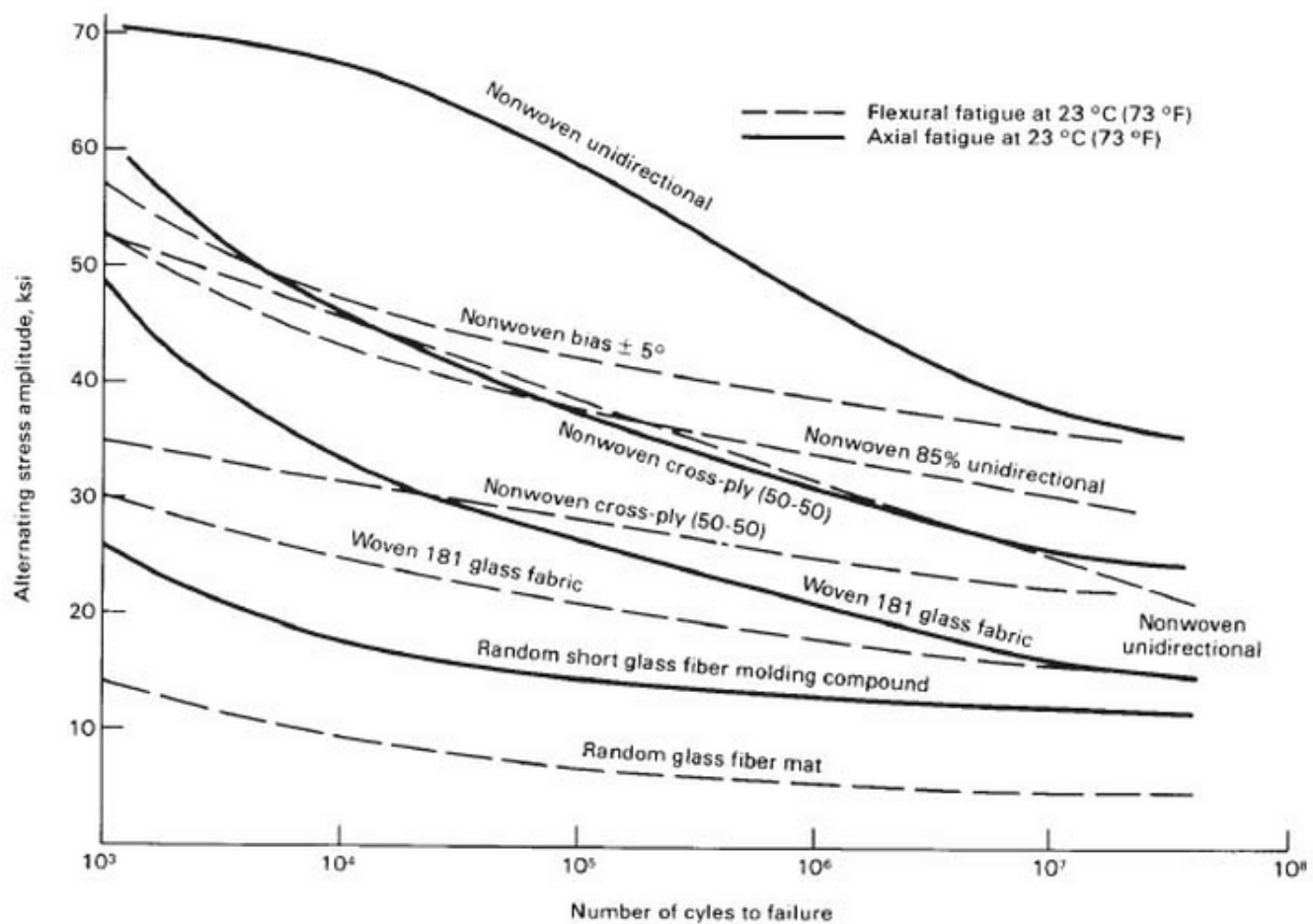


Fig. 15: s-n curve: a look at the fatigue lifespans of multiple types of fiberglass. Since the leaf springs will be bending, the stresses of import are the flexural loads, as represented by the dashed lines. All nonwoven, unidirectional fiberglass has a high fatigue lifespan (Source: ASM Engineer's Guide to Composite Materials).

- 2) **General spring shape.** From the Free-Body Diagrams drawn during the attempt at the TSSLS solution we discovered that a spring that, under load, was *parallel to the thigh* at the thigh connection and *parallel to the ground* at the boot connection would be optimal to reduce shear stresses on both connections. This resulted in a spring that would be vaguely "C-shaped" during loading, which attached to the leg with the concave side facing away from (TSSLS) or toward (TSMLS) the back of the leg.
- 3) **Required force and deflection**—these were both design criteria specified in Table I.
- 4) **Nature of thigh and shank connections.** It was known that a hinge connection at the thigh would provide the spring with all the freedom needed to bend and deform as the user squatted. It was also known that the same would be adequate for the boot connection; however, the addition of a ball-joint element somewhere in the connection could yield additional off-axis mobility for the user.

## B. Unknown Factors

- 1) **Thigh and shank connections.** Though it was roughly known how the spring would connect to the thigh and the shank, the materials to be used for the actual connecting pieces remained unknown.
  - a) *Thigh:* a few proposed designs were discussed, including using the top half of a rehabilitative knee orthosis or creating a custom connection using a formable material. A closer look at the costs of either design would determine which would be used.
  - b) *Shank:* instead of just a strap connecting the spring near the ankle, which would hinder the natural movement of the user, a standalone boot connection with an articulated ankle was proposed. This boot would have the connections discussed earlier, though the implementation of the boot remained unknown. Possible solutions included creating a boot out of aluminum, thermoplastic, and some straps. Another idea would be to use an actual boot and somehow connect it to the spring with the insertion of an additional piece.
- 2) **Two-dimensional Spring Stiffness.** Since the exoskeleton was to be a custom-built two-dimensional spring, the exact force-deformation relationship and the stiffness required to provide the required forces was a mystery. Options for resolving this included:
  - a) Theoretically characterize a spring with the desired qualities and then build it. This would likely be done with a Finite-Element Analysis (FEA) in SolidWorks. However, since the squat motions involved very large deformations, for which FEA simulations are not as accurate, this prospect seemed unattractive.
  - b) Build a few springs with different thicknesses and characterize them once the resistive forces were of similar magnitude to the desired quantities—a “guess and check” approach. Since this involved actual empirical testing, it would be more accurate, but if the prototyped springs consistently failed to give good results then another solution would have to be considered.
 

The spring could be characterized via gathering of deformation data and matching it to the vertical component of the spring’s resistive force. Using a two-dimensional form of Hooke’s Law, stiffness matrices could then be generated. This would likely be done in MATLAB with photo or video data and post-processing to find stiffness over the largest range of deformation values possible.
- 3) **Effect on muscular endurance.** As this is the whole object of the exoskeleton device, testing its effect on muscular endurance will be the greatest measure of success. This will be tested on several subjects by measuring changes in O<sub>2</sub> consumption data as well as changes in maximum possible cycles till exhaustion.
- 4) **Method for Allowing Unhindered Gait.** A mechanism had to be concocted for solving the problem of allowing the user to walk without the TSSLs providing significant spring force against the motion of walking.

## C. Standards

Since the design of the device involves mechanical components like springs and slides, not to mention the device is intended toward use in manual labor, some standards that are relevant to the design have been identified:

- 1) **OSHA**—The Occupational Safety and Health Administration is concerned with safety in health in the workplace. Since the lower-limb exoskeleton device is intended for use in any of several manual-labor workplaces such as factories, warehouses, construction sites, homes, etc, it is vital that any design decision complies with these standards.
- 2) **ASME**—The American Society of Mechanical Engineers is the leading producer of standards for mechanical engineering. Since they have grown to have over 600 standards, it is only fitting that the mechanical components of the spring comply with all of ASME's standards.
- 3) **ASSE**—The American Society of Safety Engineers is also all about protecting people from the hazards of engineering. It is absolutely essential that there are no potentially dangerous failure modes of the spring-loaded device such that it breaks one of these standards.

## V. PROTOTYPING NARRATIVE

### A. Design Evolution

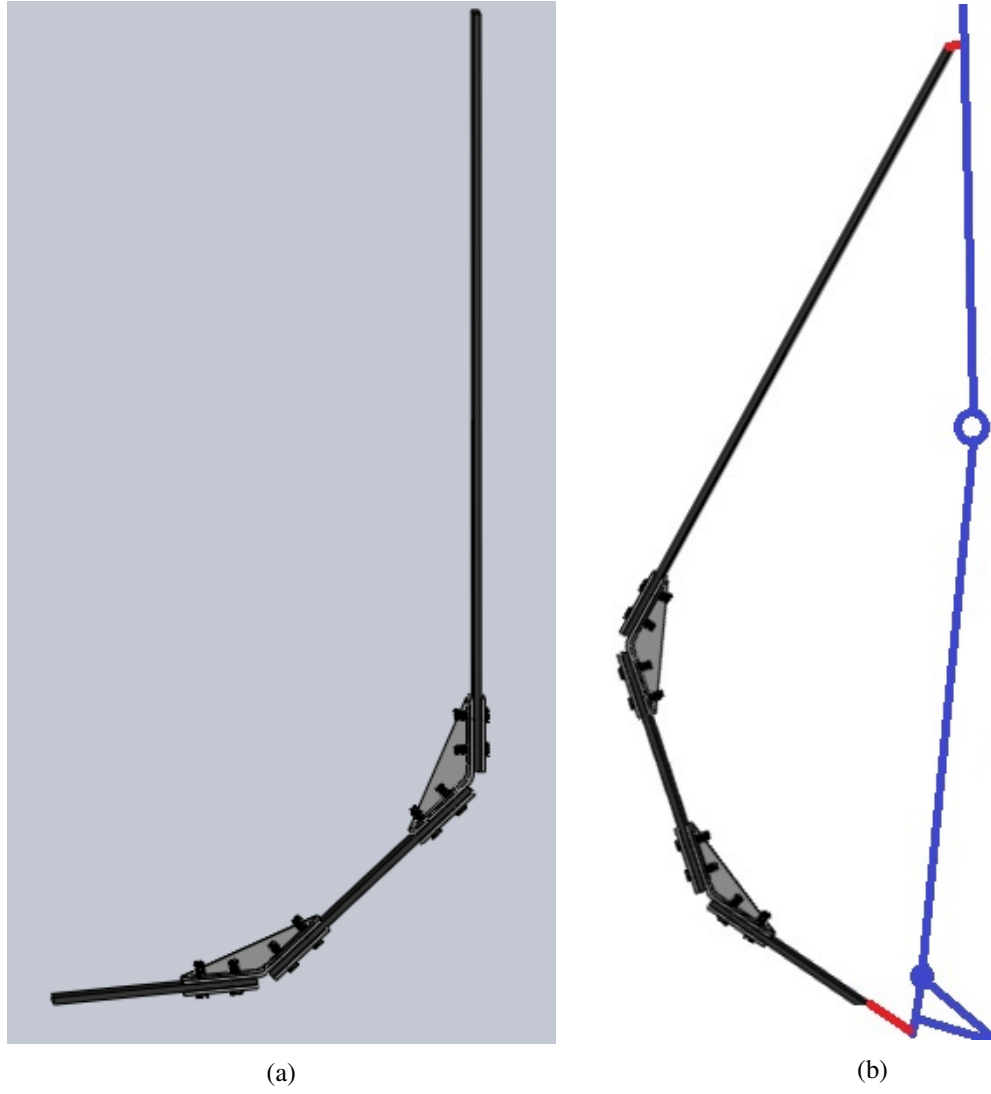


Fig. 16: (a) SolidWorks model of the TSMLS spring. (b) Intended orientation with user's leg.

*1) Leaf Springs:* The SolidWorks model for the leaf springs is shown in Fig. 16a. The three springs—to be connected in series—were designed to three different lengths: 22.3" for spring 1, 8" for spring 2, and 6" for spring 3. These lengths were chosen to give one spring a majority length to ensure that the majority of flexing would be along one rotational axis, making it easier to join to the natural rotation of a user later.

The spring connection angles were calculated with the reasoning being that under load and a full squat, the first spring should be reasonably parallel to the thigh and the third spring should be reasonably parallel to the ground. An angle of 30° was chosen here to be close without requiring that the angles between springs be much larger than 45°. The springs, once joined in series at these angles, appeared as they do in Fig. 16a.

Two different spring thicknesses were considered: .125" and .25" thick fiberglass. The thickness of the fiberglass would directly affect the stiffness and resistive force of the springs, so a thickness had to be chosen that could give enough force and still deform to the required specifications. The final chosen thickness would be decided during the prototyping stage.

Finally, a flange piece was added to the model at the connections to reinforce their strength.

A summary of the spring specifications is provided in Table VI below:

TABLE III: A summary of spring dimensions.

Dimension Type	Part	Value
Length x Width	Spring 1	6" x 2"
	Spring 2	8" x 2"
	Spring 3	22.3" x 2"
	Connector	5" x 2" (bent halfway along length)
	Pressure plate	2.5" x 2"
Connection angles	Spring 1-2	47°
	Spring 2-3	37.5°
	Spring 1 to thigh	30°
	Spring 3 to ground	30°
Stock Thicknesses Considered	Springs	1/8" and 1/5"
	Connector	1/8"
	Flanges	1/16" and 1/8"
Holes and Fasteners	Fastener	1/4" -20 thread, 7/8" long
	Hole Diameter	17/64"

To choose which thickness of fiberglass to use, a closer look at the fiberglass s-n curves (Fig. 15) was taken. Both the 1/8" and 1/5" thickness fiberglasses could easily bend to the amount required; thus, it was decided that whichever thickness could withstand the higher number of loading cycles and support the most force would be chosen. First, the normal stresses from bending during flexural loads was calculated using

$$I = \frac{1}{12}bh^3 \quad (1)$$

and

$$\sigma_{max} = \frac{|M|c}{I} \quad (2)$$

Where the maximum moment  $M$  was spring 1 under maximum loading, where the spring is assumed to be nearly parallel with the thigh and the 100 N (22.5 lbf) force per spring is perpendicular to spring 1. The calculations are summarized in table IV in Imperial units to compare directly to Fig. 15 above:

TABLE IV: Comparison of fatigue tolerances in  $1/8''$  thick and  $1/5''$  thick fiberglass.

Quantity	$1/8''$ thickness	$1/5''$ thickness
$1 b$ [in]	2	2
$h$ [in]	$1/8$	$1/4$
$I$ [ $in^4$ ]	$3.256 \cdot 10^{-4}$	$2.604 \cdot 10^{-3}$
$M$ [ $kips \cdot in$ ]	501.3	501.3
$c$ [in]	$1/16$	$1/18$
$\sigma_{max}$ [ksi]	96249.6	24062.4
Cycles to Failure	0	$\geq 10^7$

Though the  $1/8''$  fiberglass had withstood an initial one or two test deformations of one squat distance, it was clear that the reaction force given was much smaller than the desired 100 N used in the moment calculation, and loading it with 100 N would cause immediate failure. The  $1/5''$  fiberglass, in contrast, could withstand more than  $10^7$  cycles of 100 N load if made out of any non-woven, unidirectional fiberglass.

2) *Thigh Connection:* The thigh connection to the spring was to be constructed from thermoplastic—namely, a high-strength glass-strengthened polycarbonate that is easily thermoformed. The connection to the spring is to be a simple hinge connection, as shown in Fig. 17. Finally, straps were inserted through slots in the molded thermoplastic so that the user can strap the device to the leg, and adhesive-back foam was added to the inside of the mold for increased comfort.

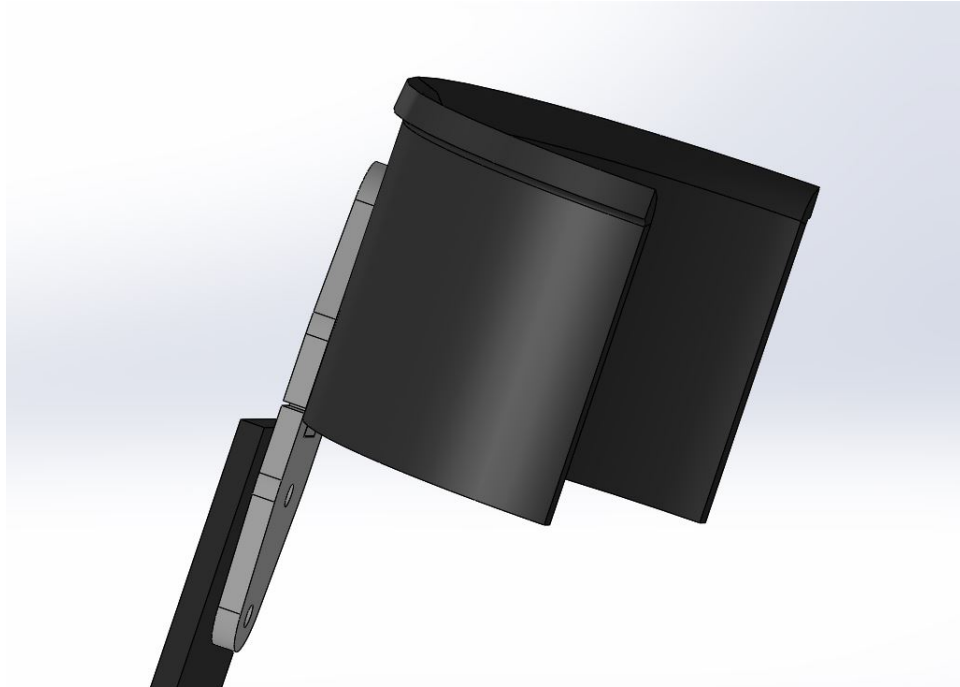


Fig. 17: The thigh connection to the spring.

The connection has a simple one-dimensional rotational degree of freedom. When the user bends and deforms the spring, it swings along the hinge.

The specifications of the thigh connection are summarized below in Table V:

TABLE V: A summary of thigh connection dimensions.

Part	Dimension	Value
Polycarbonate	Length	10"
	Width	4"
	Thickness	1/4"
Adhesive-backed foam	Length	10"
	Width	4"
	Thickness	1/4"
Fasteners	Number of Fasteners	4
	Thread Size	1/4" - 20
	Length	7/8"

3) *Boot Connection:* From its other projects the Biomechatronics group at the MIT Media Lab found itself in possession of an unused pair of combat boots. These boots had been retrofitted with a carbon fiber piece through the soles, which was perfect for a spring attachment. The connection to the carbon fiber piece meant that any stresses on the connection from the spring would be transferred into the sole of the boot rather than the ankle of the user.

The boot was to be connected to the spring via a hinge connection, which would allow the ankle to rotate, as well as the spring to swing back and accommodate the rotation of the thigh during a squatting motion (Fig. 18)



Fig. 18: The combat boot.

The specifications of the boot connection are summarized below:

TABLE VI: A summary of boot connection dimensions.

<b>Part</b>	<b>Dimension</b>	<b>Value</b>
Carbon Fiber Piece	Thickness	.2"
	Width	2.25"
	Angle from horizontal	61°
Boot	Shoe Size	US 12

4) *Hinges:* Two types of hinges were considered for inclusion in the TSMLS device: steel strap hinges and steel strut hinges. The strap hinges were smaller and lighter, with a 360° range of motion. The strut hinges were larger and heavier and had a 270° range of motion. The trade-off between strength and weight was a difficult one to make because a lightweight device was one of the main advantages of a passive elastic system, but the hinge connections were also critical components where failure would be undesirable, which required a high factor of safety.

A Finite-Element-Analysis simulation was performed on the strap hinges to determine if they were strong enough to the device. Fixing the geometry bound to the thigh or boot connection and adding the bearing loads from the fasteners connected to the springs, the simulation gave a Factor of Safety of about 1.5 (Fig. 19).

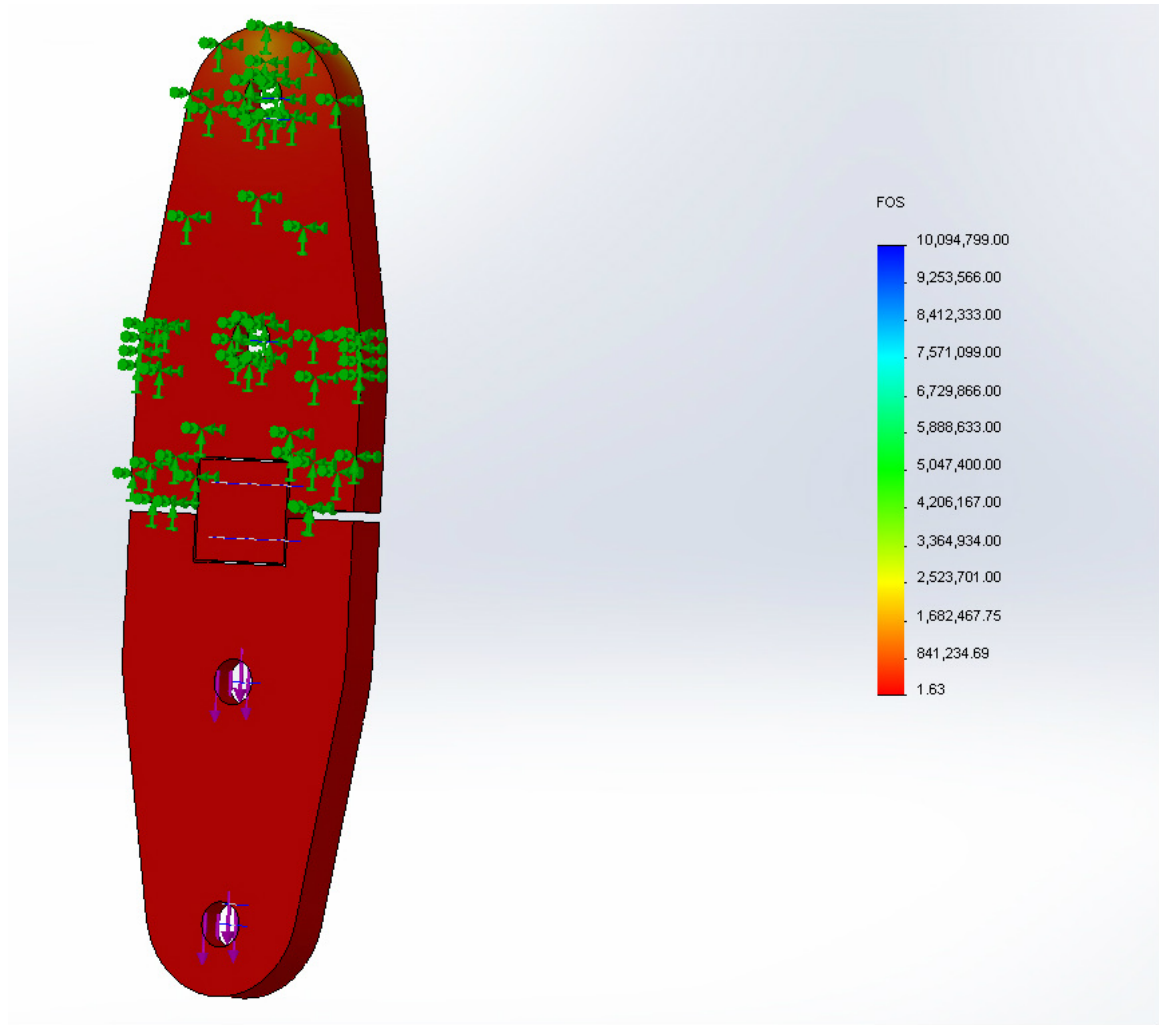


Fig. 19: Finite Element Analysis of the strap hinge.

The strut hinges were chosen over the strap hinges because their additional thickness would provide a higher factor of safety (see Appendix B).

5) *Combining:* The SolidWorks model of the entire connected exoskeleton is pictured below in Fig. 20.



Fig. 20: The completed design of the exoskeleton.

## B. Fabrication and Redesign

1) *Leaf Springs:* The fiberglass leaf springs were cut on a band saw to the specifications mentioned in Table VI. The cut pieces can be seen in Fig. 21—after cutting on the band saw, stray fibers were sanded off on a belt sander.

The connectors were cut from .125" thick aluminum, also on the band saw, and were bent to the desired angles by clamping them in a vise and manually bending them, checking the angle of the bend with a protractor. The bending force was applied as close to the vise as possible to ensure the bend was angular and not rounded. The pressure-distributing plates were also cut on the band saw from .125" thick aluminum.

17/64"-diameter holes were drilled into the springs, then those holes were used as a template to place the holes on the connectors and the pressure plates to ensure good hole alignment.

The profiles of the flanges were drawn from the profile of the bent connectors to ensure a good fit. They were cut on the band saw from .125" aluminum and attached to the connectors with SteelStik<sup>©</sup> epoxy. The connection was roughed using a steel brush and cleaned with ethanol; still, upon initial loading the flange promptly failed and disconnected—a new approach had to be designed.

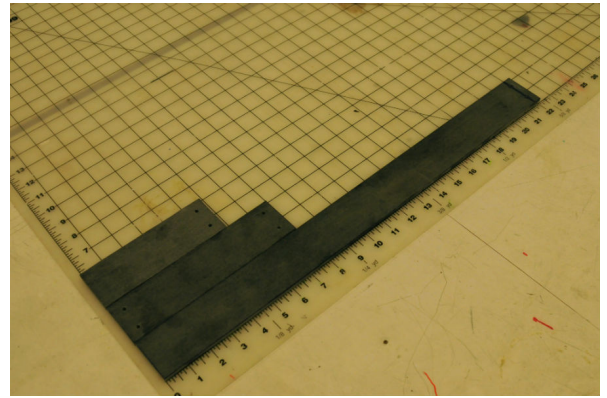


Fig. 21: A view of each leaf spring before assembly.

The connectors were cut from .125" thick aluminum.

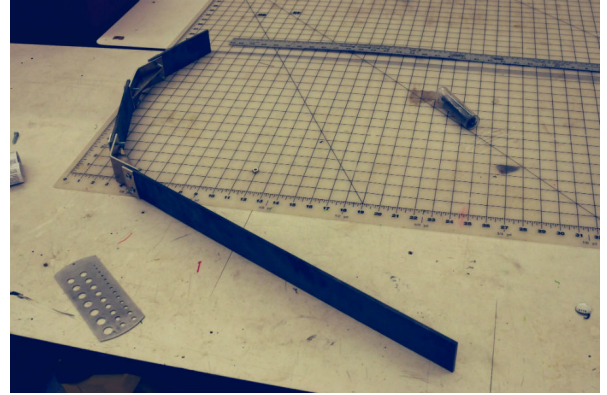


Fig. 22: A view of the spring after assembly.



(a)



(b)

Fig. 23: Trouble with flange attachments.(a) Upon epoxying, (b) upon failure.

The new flange design incorporated aluminum stock that was half as thick, 0.0625", with the idea that two would be used. Each pair of flanges would still have the triangular section with the addition of formed

“tabs” that the fasteners could go through, adding strength and eliminating the chance of the flange falling off.

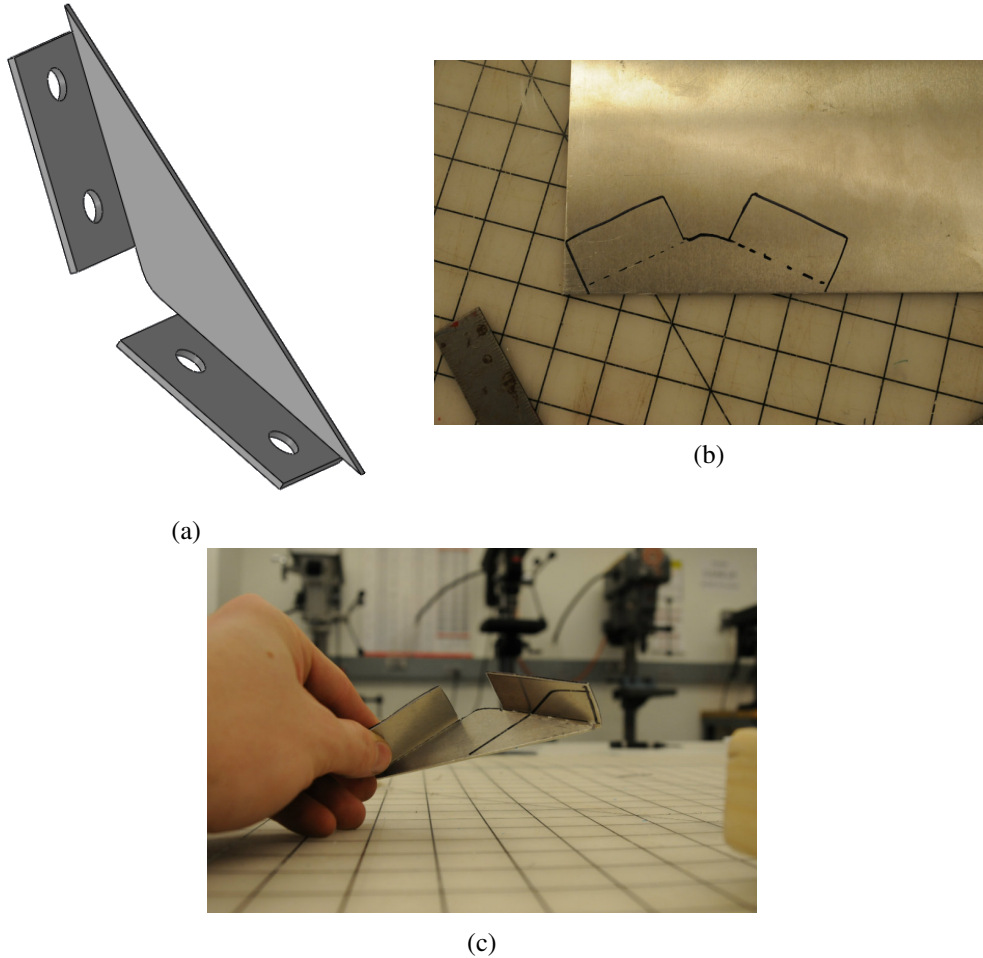


**Fig. 24:** New flange attachments: (a) SolidWorks model of the new flange piece, (b) flat profile before band saw and bending, (c) the shaped flange before hole addition.

Finally, four more holes were drilled on the distal ends of spring 1 and spring 3. These would be used to connect to the hinge that attached the thigh and boot pieces to the device.

A total of 24 fasteners was used per spring. These were 1/4"-20 thread low-profile alloy steel socket head cap screws with a length of 7/8" each.

2) *Thigh Connection:* As seen in Fig. 25, the thigh connection is built from high-strength glass-reinforced polycarbonate, which is a thermoform plastic capable of withstanding heavy loads and is easily formable with a heat gun.

First, the 1/2" thick sheet of polycarbonate was milled to a thickness of 1/4". It was then cut into two pieces that were 10" long by 4" wide (the back half of the circumference of the author's thigh was measured to be about 10"). Using a heat gun, the polycarbonate pieces were molded to the shape of the back of the thigh.

To make the connection more comfortable, the inside of each polycarbonate piece was fitted with a 0.25" thick piece of adhesive-backed foam. The foam was chosen to be soft and resistant to water damage that would come from any sweating of the user.

To connect this piece to the leg, two slots were cut on either side of the piece, and two velcro clinching straps were inserted through these slots. Finally, four holes were drilled into the back of the completed thigh piece, and it was attached to the spring via a hinge connection.

3) *Boot Connection:* Four holes were drilled into the angled part of the carbon fiber piece. The hinge was connected to this part, which then attached to the spring, as shown in Fig. 26.



Fig. 25: The thigh connection, attached to the spring. The hinge is visible on the back.



Fig. 26: The boot connection to the spring.

4) *Hinges*: The strut hinges' extra length on either end was sawed off using the band saw. Four addition holes that fit the dimensions of the thigh and boot connections, as well as the holes on spring 1 and 3, were drilled. The results can be seen on the previous figure.

5) *Combining*: Once fully fabricated, the exoskeleton could be worn as shown in Fig. 27.



Fig. 27: How to wear the exoskeleton.

With the exoskeletons fully prototyped, two types of experiments were performed: spring characterization to understand spring stiffness during loading and construct a reference of forces, and metabolic testing that would not only use that reference to calculate force and energy storage but also test the exoskeleton's metabolic advantage during squatting exercises. These experiments will be explored fully in the following sections.

## VI. SPRING CHARACTERIZATION

In order to understand how the spring would behave while deformed and to characterize its stiffness, an experiment was designed and performed using a force sensor and a video camera above the spring. Clenched in a vice, the spring deformed when pulled by the experimenter's hand via a handle attached to a force sensor. The sensor recorded force data, and the video could be used later to interpolate spring deformation and angle of force. The stiffness and force values could then provide a reference for calculating force and energy storage during metabolic squat testing, which was pivotal to evaluating the device against the design criteria.

### A. Experimental Design

The force sensor recorded force in Newtons at a sampling rate of 250 Hz. This force sensor was attached to a handle on one side and a length of nynon string on the other. The nylon spring was wrapped around the thigh-end of the spring, which was then placed horizontally in a vise, which clamped the boot-end of the spring—this simulated the motion of the user's thigh while their feet remain planted and stationary (Fig 29).

A video camera was placed on a tripod above the vise and spring with the lens facing down. A white posterboard was placed under the spring to enhance the contrast in the video. In order to understand the pixel-to-distance ratio in the video image, a set of calipers was placed in frame, set to a distance of 5 in.

Two trials were performed of the experiment, during which the experimenter grabbed the force sensor and deformed the spring in a multitude of arcs over a time of roughly one minute. During the beginning and end of each trial, the experimenter gave a sharp impulse to the spring while holding the spring—those impulses would appear as sharp spikes in the force data, which served as reference points to sync the force data to the video data.

Once the video data from both trials had been collected, they could be imported into MATLAB and processed using MATLAB's Computer Vision Toolkit. A simple point tracking algorithm was used to track the thigh-end of the spring as it deformed throughout the test. A coordinate system was created with the  $x$  and  $y$  direction as shown in Fig. 30. The green points that dot the figure are all the available points for tracking, and the red points are the ones chosen to track. The origin of the coordinated system was defined as the spring's original location, at  $t = 0s$ .

Another point to be tracked was the force sensor itself—by constructing a vector between the spring and the sensor, the angle of applied force could be determined (the red line in Fig. 30).



Fig. 28: The force sensor.

## B. Least-Squares Analysis of Stiffness Matrices

In order to characterize two-dimensional stiffness for all the data, the stiffness matrices for each frame of data must be derived. In two dimensions, stiffness obeys the equation below.

$$\begin{bmatrix} dF_x \\ dF_y \end{bmatrix} = \begin{bmatrix} K_{xx} & K_{xy} \\ K_{yx} & K_{yy} \end{bmatrix} \begin{bmatrix} dx \\ dy \end{bmatrix} \quad (3)$$

In two dimensions, stiffness takes the form of a 2x2 matrix. This includes two principle stiffnesses,  $K_{xx}$  and  $K_{yy}$ , as well as two off-axis stiffness terms,  $K_{xy}$  and  $K_{yx}$ . According to the Maxwell's Reciprocity Theorem, the off-axis stiffnesses  $K_{xy} = K_{yx}$  [23], which was renamed  $K_\theta$ .

The matrix equates takes a differential form because the stiffness matrix is not constant; rather,  $K$  is actually a nonlinear function of both  $x$  and  $y$ . Therefore, each matrix is valid only for a small deformation  $dx$  and  $dy$  that causes some small reaction force  $dF_x$  and  $dF_y$ . For each point along a deformation arc, a new stiffness matrix must be calculated. Also, even with the simplified off-axis stiffnesses there are still too many unknowns for these two linear equations to be able to solve. This necessitates a statistical approach to solving stiffness.

As displayed in Fig. 31, by taking multiple data points a least-squares analysis could be performed for stiffness. At any local point B in the deformation data, two nearby reference points A and C could be taken. If these are close enough to the reference point, these could be considered to be "small perturbations" from B. For such small perturbations, the stiffness matrix K could be considered constant with little error. This allowed two sets of two equations to be taken with only three unknowns, reformed into the general least-squares form  $Y = X\beta$  as in Equation (4). The  $\beta$  matrix in this case is a reshaped stiffness matrix that is a statistical estimator of stiffness.

$$\begin{bmatrix} dF_{x_{ab}} \\ dF_{y_{ab}} \\ dF_{x_{cb}} \\ dF_{y_{cb}} \end{bmatrix} = \begin{bmatrix} dx_{ba} & dy_{ba} & 0 \\ 0 & dx_{ba} & dy_{ba} \\ dx_{cb} & dy_{cb} & 0 \\ 0 & dx_{cb} & dy_{cb} \end{bmatrix} \begin{bmatrix} K_{xx} \\ K_\theta \\ K_{yy} \end{bmatrix} \quad (4)$$



Fig. 29: The spring, clamped in the vise.

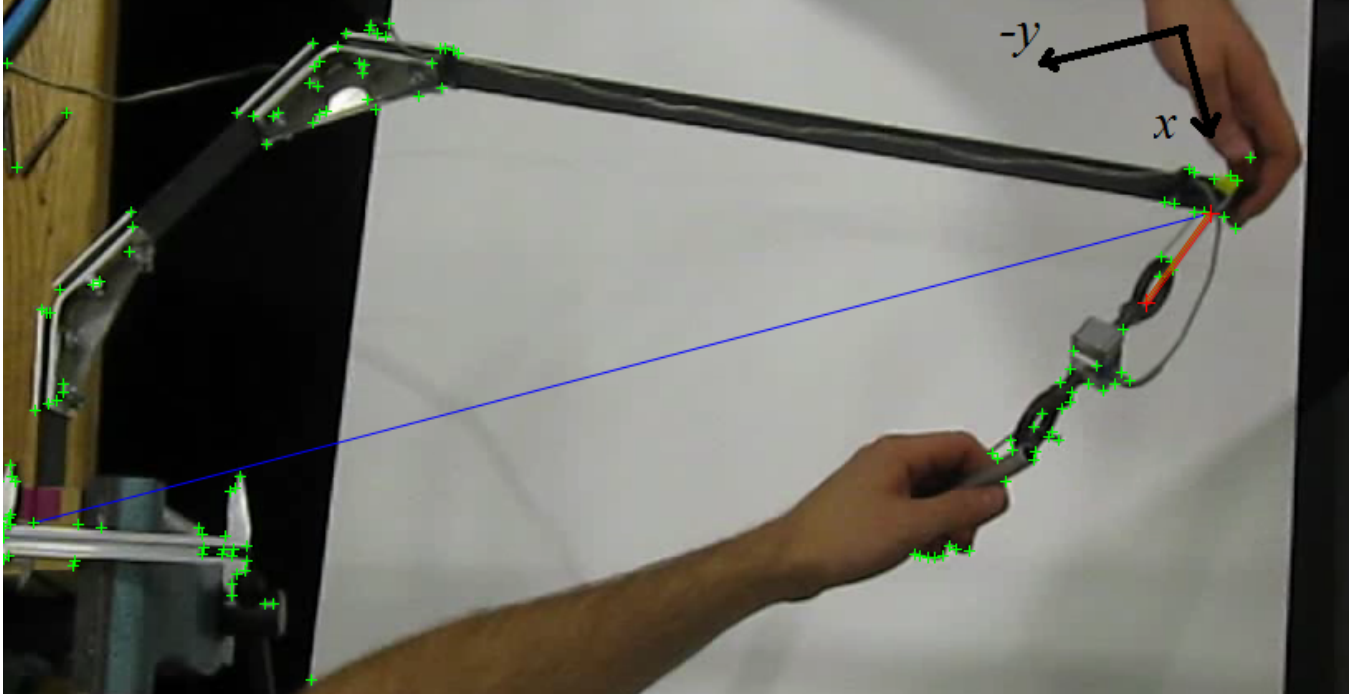


Fig. 30: A visualization of MATLAB's point-tracking algorithm. The two tracked points are the two endpoints of the red vector, which defines the angle of applied force.

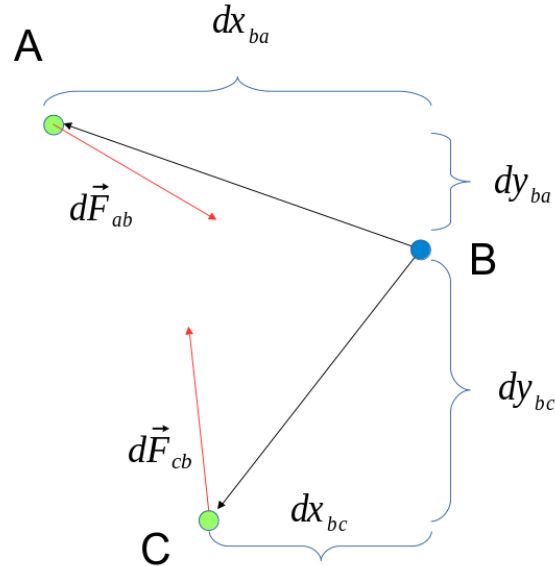


Fig. 31: A visualization of the least-squares analysis.

$$Y = X \beta$$

Once the equations had been gathered, the estimator  $\beta$  could be found by

$$\beta = (X^T X)^{-1} X^T Y \quad (5)$$

However, finding a good system for taking reference points proved difficult. The time resolution of

the video data was 30 frames per second, and as such three *sequential* points were often not linearly independent. This led to negative principle stiffnesses, which is physically impossible.

This led to a new system of comparing sets of three points: while iterating through every frame of data, two points were chosen to compare to it: one with a sufficient  $x$  distance, and one with a sufficient  $y$  distance. Arbitrary (though necessarily small) threshold values were set for these distances, and the point could be from any other frame of data—because of this, points became much more likely to be linearly independent and yielded better stiffness values.

The accuracy of the estimated stiffness values can be measured by taking the Root Mean Square Error (RMSE) of the measured  $Y$  force matrices against those calculated by  $X \times B$ . Another metric is to use the percent error of the absolute values of the differences between those values. The results of the spring characterization tests and the estimated stiffness values will be discussed in detail in the Results section.

## VII. EXOSKELETON TESTING ON METABOLIC DATA

### A. Experimental Design

The metabolic squat tests were performed on two subjects, each of approximately 800 N in weight and over 1.82 m (6'0") in height. These subjects underwent two six-minute trials during which they performed one squat every three seconds (Fig 32a). One test was performed with the exoskeleton, and the other was performed without the exoskeleton as a control. The metabolic data from both tests, which included  $O_2$  consumption and  $CO_2$  generation, were recorded with the COSMED metabolic data acquisition system (Fig. 32b).



Fig. 32: (a) Metabolic testing. (b) Setup of the COSMED system for metabolic data acquisition.

To make sure any measured metabolic effects were not simply the result of one trial being first, Test Subject One underwent the control trial first, and Subject Two underwent the exoskeleton trial first. A metronome was used to ensure proper timing of squats, and a length of string tied around the subject was used to ensure a consistent squat depth. The length of the string was adjusted such that at a full squat depth, the string touched the ground. Finally, the deformation data was acquired using the same video capture and computer vision algorithms used in the spring characterization. This data would later be compared to the characterization data to calculate stiffness and force, as well as energy storage and release.

This COSMED system was rigorously calibrated to produce accurate results. First, the ambient air was tested as an input. Next, the detection of air composition was calibrated using a known reference gas mixture. The flowrate through the COSMED's turbine was then calibrated by ventilating a syringe of known 3 L volume. Finally, evenly timed breath calibration was performed, and the air humidity was entered.

Metabolic data can be equated to energy expenditure using the standard gas exchange equation [24]:

$$\text{Energy expenditure (kJ)} = 16.58O_2 + 4.51CO_2 - 5.90N \quad (6)$$

Where  $O_2$  is the Oxygen consumption,  $CO_2$  is the Carbon Dioxide generation, and  $N$  is the excreted urinary Nitrogen. The Nitrogen term can usually be corrected for in the COSMED software, and only the first two terms are necessary to gather. Of the six minutes in the trials, the last two are taken as representative of the endurance exercise.

Once the energy consumption in kJ was calculated, it was normalized with respect to time and body mass. This became the normalized power consumption, in units of  $[W/kg]$ . Both the control and exoskeleton trial had an associated specific power consumption,  $P_{control}$  and  $P_{exo}$ , that were calculated in this manner. In addition, the baseline metabolic cost of standing,  $P_{standing}$ , was calculated. These expenditures were combined as such to find the percent change in metabolic power consumption due to the exoskeleton:

$$\text{Percent change} = \frac{(P_{exo} - P_{control})}{(P_{control} - P_{standing})} \times 100 \quad (7)$$

If  $P_{exo} < P_{control}$ , the percent change is negative, indicating a metabolic advantage.

## B. Shifting the Coordinate System

The hinge in the boot connection created a different style of deformation than during the stiffness characterization, which utilized a clamping vise. The coordinate system of the squat tests was therefore shifted by the spring's length swinging about the boot hinge—to correct for this, the angle of the boot hinge was tracked for each frame of data in MATLAB, and the deformations were transformed to the position they would have been in if the hinge had stayed rigid (Fig. 33).

Once the coordinate system had been shifted into the system of the characterization data, the deformations could be compared directly, and stiffness could be extrapolated and force calculated. The true force could then be found by re-shifting the coordinate system into the squat-test system.



Fig. 33: Shifting the coordinate system. The two green lines indicate the distance from boot to thigh connection—the line terminating with the red '+' sign is unshifted. Blue '+' is shifted. The line in the lower right tracks the angle of the boot hinge.

### C. Stiffness Extrapolation

Once in the characterization data's coordinate system, the deformation data from the squat test were compared to that from the characterization (Fig. 34).

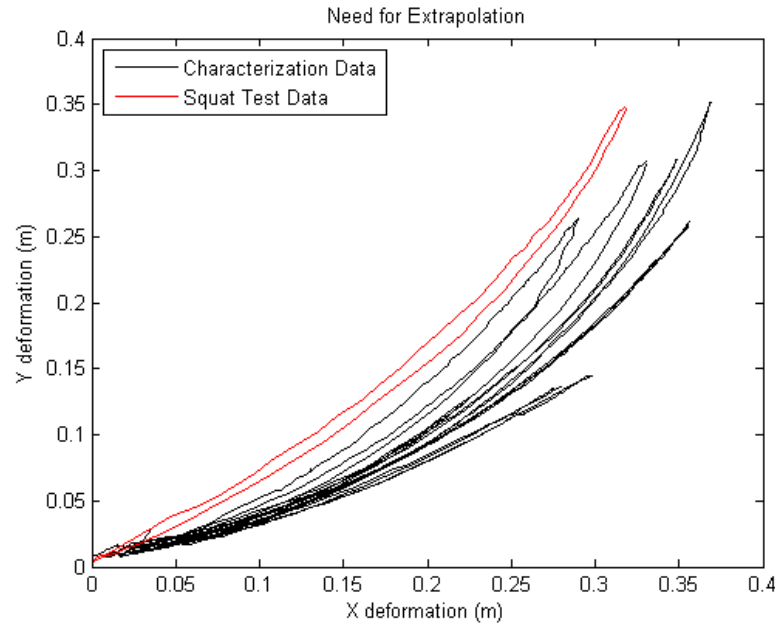


Fig. 34: Comparing squat-test deformations (red) to characterization deformations (black). Though the ranges and paths traveled by the spring are close, they are not an exact match.

Though it traveled in a very similar arc and along very similar values compared to the characterization data, the squat test deformations did not *perfectly* trace any of these arcs. To find the spring stiffness here, a two-dimensional extrapolation was performed.

The  $x$ -component and  $y$ -component deformations of each characterization arc were separated and superimposed on one another in two composite deformation groups. Each stiffness value from characterization,  $K_{xx}$ ,  $K_{yy}$ , and  $K_\theta$ , were taken as functions of both  $x$  and  $y$ . These were all used as inputs in MATLAB's two-dimensional extrapolation function *griddata*. Using the new deformations as additional inputs, vectors were created containing the extrapolated stiffness values. Because all input vectors were in the time domain, the difference between loading and unloading was preserved—that is, the loading segment of the squat test deformation data used the characterization's stiffness and deformation data from loading, and unloading used that from unloading. In this way the difference in resultant force between loading and unloading was maintained and later quantified in terms of energy loss, or damping, during a squat cycle.

## D. Calculating Force

Once squat-test stiffness had been extrapolated, calculations for force could be performed. Since the linear equations contained in the matrix Equation (3) were in differential form,  $x$  and  $y$  forces were calculated by integrating over every frame of data:

$$F_x = \int K_{xx} dx + \int K_\theta dy \quad (8)$$

$$F_y = \int K_\theta dx + \int K_{yy} dy \quad (9)$$

## E. Calculating Energy Storage and Release

The force components, along with the  $x$  and  $y$  deformations, can be combined to create two vectors:

$$\mathbf{F} = \langle F_x, F_y \rangle \quad (10)$$

$$\mathbf{s} = \langle x, y \rangle \quad (11)$$

The full squat can be divided into two main segments: loading and unloading. If the loading segment of the squat occurs from some points  $a$  to  $b$  and unloading from some points  $b$  to  $c$ , then the energy stored in each spring in the form of work is equal to the dot product of the force and deformation vectors from  $a$  to  $b$ :

$$\text{Energy stored} = \int_a^b \mathbf{F} \cdot d\mathbf{s} \quad (12)$$

which becomes

$$E_{stored} = \int_a^b |F| \cos(\theta) ds \quad (13)$$

Where  $\theta$  is the angle between the force and deformation vectors. In a similar manner, energy released can be calculated as

$$E_{released} = \int_b^c |F| \cos(\theta) ds \quad (14)$$

The percent damping of the system is then

$$\text{Percent damping} = \frac{E_{stored} - E_{released}}{E_{stored}} \times 100 \quad (15)$$

It was clear that the characterization data was an invaluable reference for the squat tests. From measuring only deformation, many quantities such as stiffness, force, energy, and damping could all be calculated.

## VIII. RESULTS

### A. Stiffness Characterization Data

The force and deformation data obtained during both trials are displayed in Fig. 35. From the tests we see that the maximum force from the spring was 165 N, which when paired with a second spring from the other leg is well over the 200 N goal (Table I). Similarly, the total ( $x$  and  $y$ ) deformation is 0.51 m, which is much greater than the 0.3 m needed during a squat.

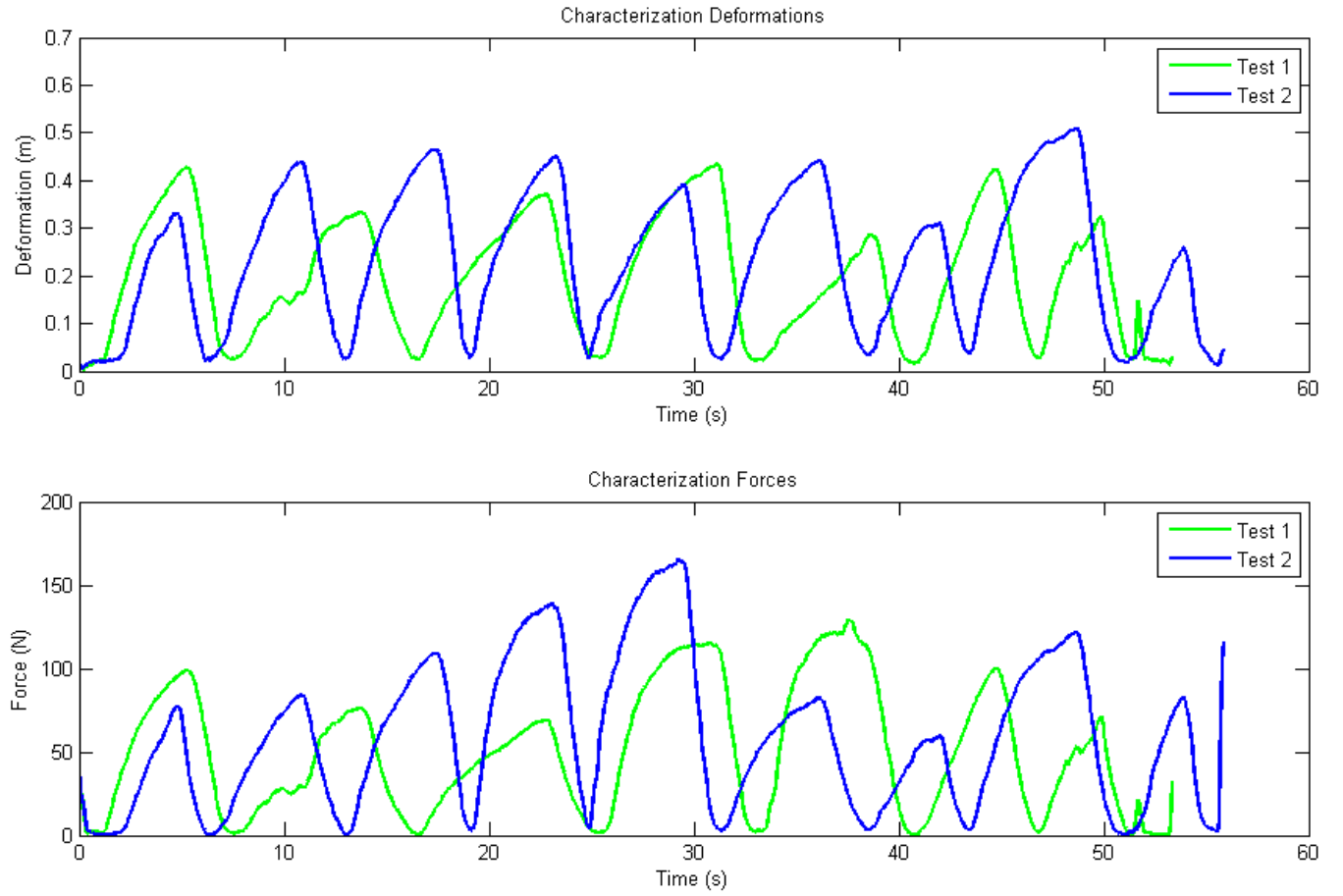


Fig. 35: The force and deformation data for both tests.

Again, it must be noted that the boot-end of the spring was clamped in a vise during the characterization testing instead of using a hinge joint like the finished device. This was done for safety reasons to prevent any accidental unleashing of the spring's force on the experimenters.

The accuracy tests of the estimated stiffness values was unusually high at first. However, the vast majority of the error occurred at the local extrema of the deformation arcs. This is because the differential deformation and force values were very close to zero, significantly reducing the signal-to-noise ratio. Telltale signs of this error are negative values for principle stiffnesses  $K_{xx}$  and  $K_{yy}$ , which are physically impossible (Fig 36).

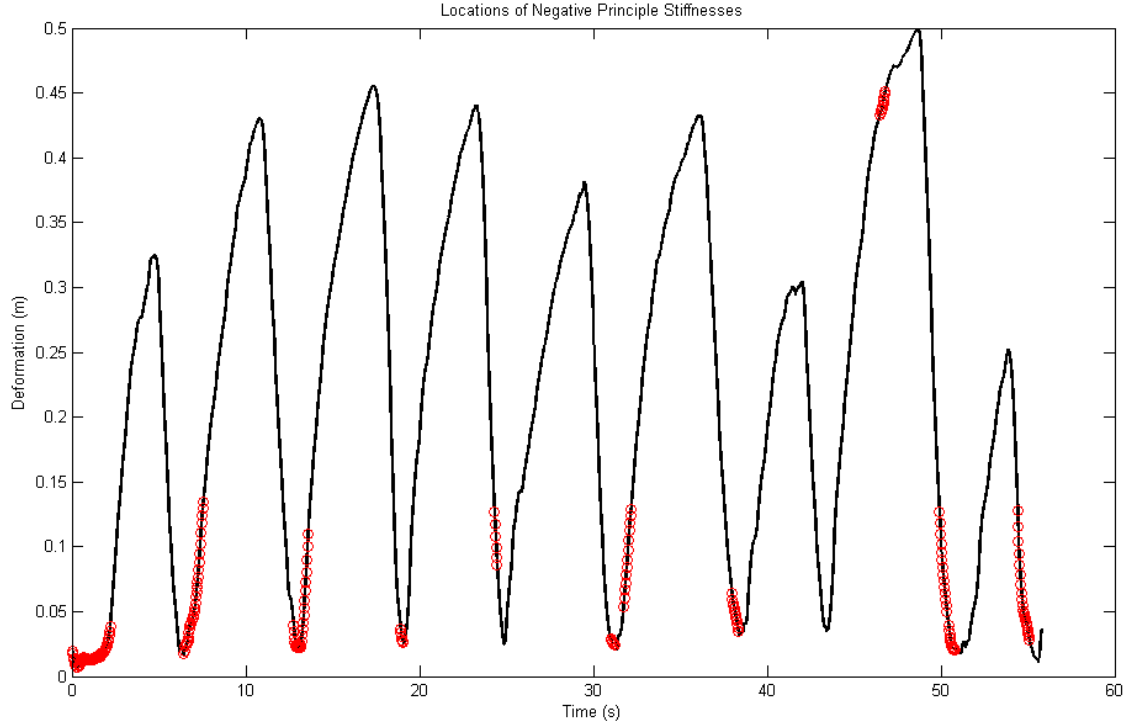


Fig. 36: The locations of negative principle stiffnesses in trial 2.

By removing this small portion of the data, error was vastly reduced, as summarized in Table VII.

TABLE VII: The accuracy of stiffness matrix estimation.

Quantity	Value
RMSE	3.63 N
Mean Percent Error	9.69%
Standard Deviation	18.86%

An intuitive way to visualize stiffness in two dimensions—more intuitive than simply plotting stiffness values over time on a graph—is through the use of the eigenvectors and eigenvalues of the stiffness matrix. These are the vectors that satisfy the equation

$$K\nu = \lambda\nu \quad (16)$$

An ellipse can be drawn using the two eigenvectors as its major and minor axis (Fig. 37). Because the stiffness matrix is nothing more than a scalar transformation of these eigenvectors, they represent the axes of stiffness in two dimensions. This is different from representing the  $x$  or  $y$  axes of a coordinate system; they are the axes of stiffness itself. For example, if a deformation occurred in the direction of one of these axes, the spring would give a reactive force in that parallel (or antiparallel) direction. In other words, the eigenvectors describe the special cases for which stiffness can be considered one-dimensional (though still nonlinear).

The off-axis stiffness term  $K_\theta$  is contained twice in the stiffness matrix, making it symmetric, and is therefore incorporated into both eigenvectors, determining the tilt of the ellipse and creating orthogonal eigenvectors.

Using this idea, the stiffness eigenvalues for both trials were plotted as vectors defining an ellipse and overlayed onto the original video files, creating new videos that provide an intuitive indication of stiffness over the course of the trials. A representative image from such a video is displayed below in Fig 38.

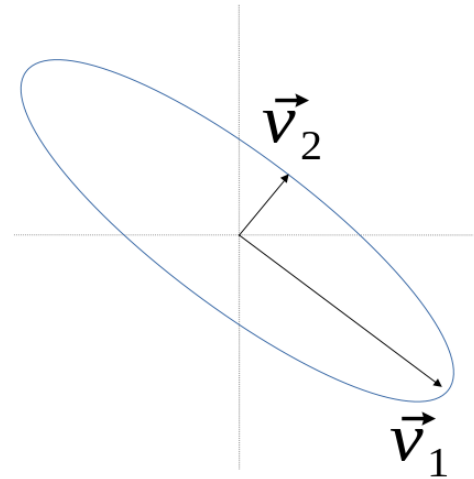


Fig. 37: Formation of an ellipse through eigenvectors.

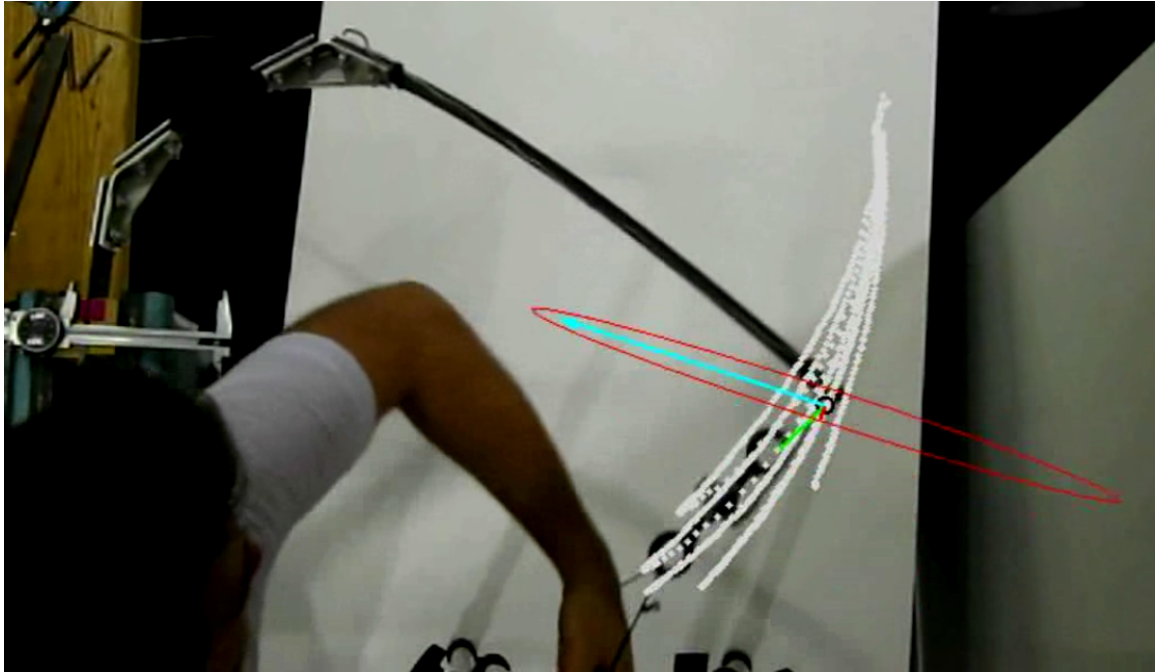


Fig. 38: Visualization of stiffness via eigen-ellipses. Here, the green vector represents the applied force, and the cyan and red vectors (scaled) represent the principle and off-axis stiffnesses.

The white lines represent the different paths traced by the spring over its many arcs back and forth under applied load. As shown by the shape of the ellipse, the spring is much more stiff in the  $y$  direction (cyan) than the  $x$  direction (red)—this is a good sign, since the user will deform the spring in the  $y$  direction while squatting.

## B. Metabolic Advantage

The COSMED software produces results of the following form (Fig. 39):

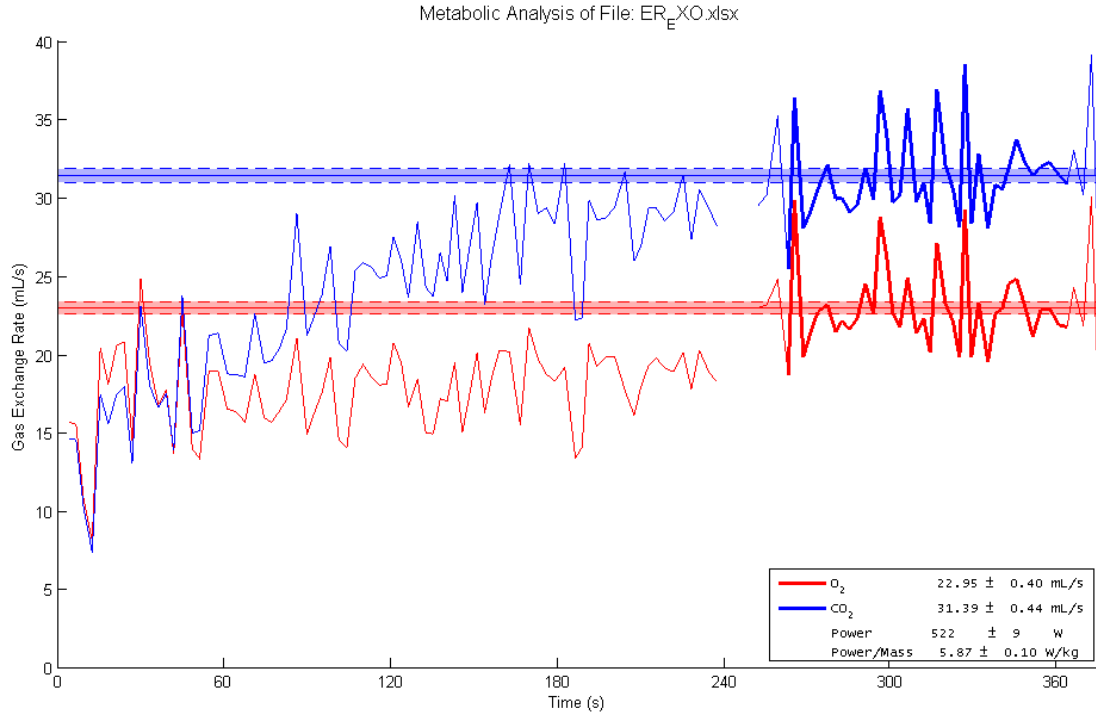


Fig. 39: Metabolic data by COSMED. The bolded segment is the window chosen to compute specific power consumption.

This is the exoskeleton trial data for Subject Two. Red indicates  $O_2$  consumption and blue is  $CO_2$  generation –the bolded horizontal lines represent the mean values for the chosen windows (when energy consumption had plateaued), and the width of those lines represents the tolerance. The graphs for all other trials and specific power consumptions were collected and computed in a similar manner, and power was computer in the same way. The specific power consumptions are listed below in Table VIII along with the metabolic advantages obtained using Equation (6).

TABLE VIII: The accuracy of stiffness matrix estimation.

Quantity	Subject 1	Subject 2
$P_{exo} [W/kg]$	$6.66 \pm 0.18$	$5.87 \pm 0.10$
$P_{control} [W/kg]$	$7.44 \pm 0.09$	$6.39 \pm 0.15$
$P_{standing} [W/kg]$	$1.64 \pm 0.09$	$1.32 \pm 0.13$
Percent Augmentation	$13.45 \pm 4.65\%$	$10.26 \pm 4.87\%$

### C. Calculating Squat Test Force

The  $x$  and  $y$  force and deformation profiles of the squat test are displayed below in Fig. 40.

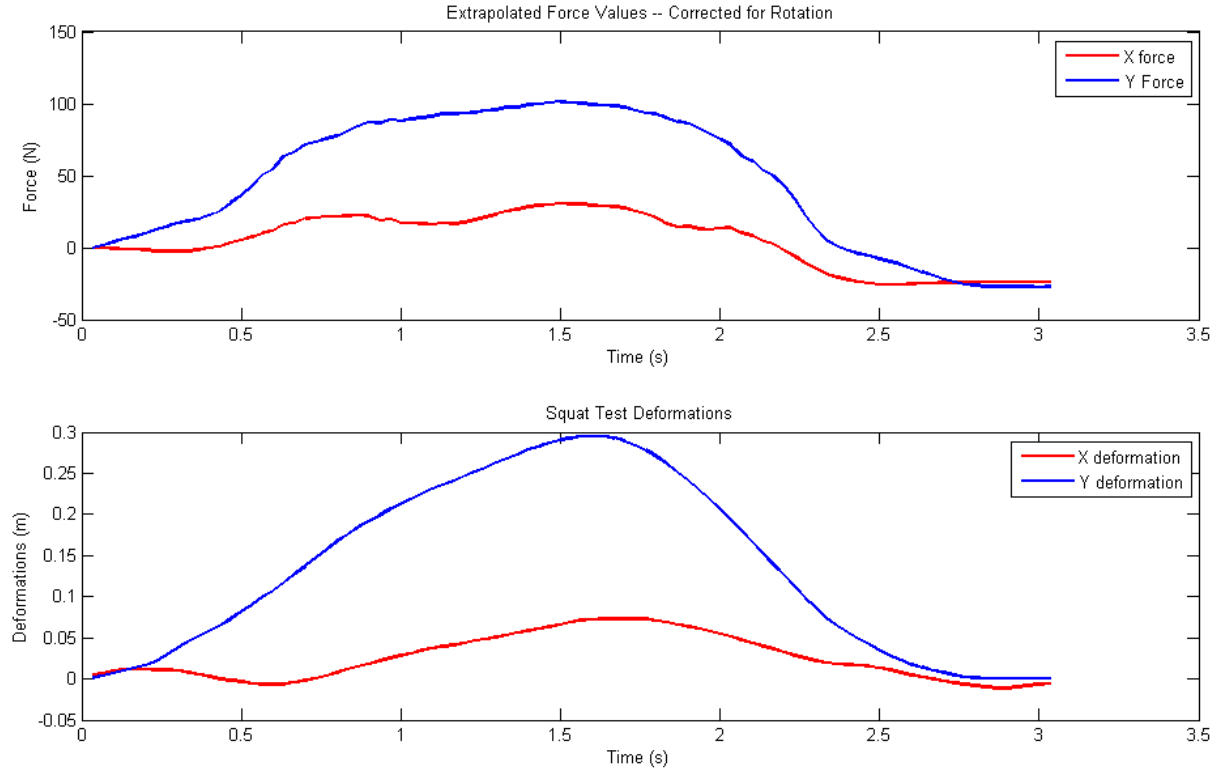


Fig. 40: The force and deformation profiles of the squat test. These have been rotated, extrapolated, integrated, and re-rotated from the squat deformation data.

The *maximum force in the y-component* is 101.36 N, meeting the required 100 N per spring. The deformation is also 0.295 m *in the y component*, almost exactly the desired squat depth accommodation. It is no surprise that the force delivered by the spring is almost entirely in the y-component: because of the boot hinge's swinging to accommodate the motion of the squat, any shear forces against the leg in the x-direction have been eliminated, making the TSMLS a comfortable device. These results are summarized in Table IX.

TABLE IX: Squat test calculated forces and deformations.

Quantity	Value
Max $y$ Force	101.36 N
Max $y$ Deformation	0.295 m

As with the characterization data, the squat test stiffnesses were visualized with ellipses and superimposed on the squat-test video data to create a video that provided an intuitive representation of the axes of stiffness. A representative frame of that video is shown below in Fig. 42:



Fig. 41: Ellipse visualizations of the squat tests. The force is represented by the green vector, and the red ellipse is defined by the eigenvalues and eigenvectors of the stiffness matrices.

The major axis of stiffness, as defined by the major axis of the ellipse, coincided almost perfectly with the  $y$  axis of deformation. This shows that the spring was designed effectively to provide an almost purely upward force during squatting. The forces and stiffness in the  $x$  direction were very small and demonstrate that the exoskeleton does not provide any substantial shear force that would cause the thigh connection to slide back and forth on the leg or cause discomfort. This is a good sign.

## D. Energy Storage, Release, and Damping

The energy storage and release calculated with Equations (13) and (14) are displayed below in Fig. 42:

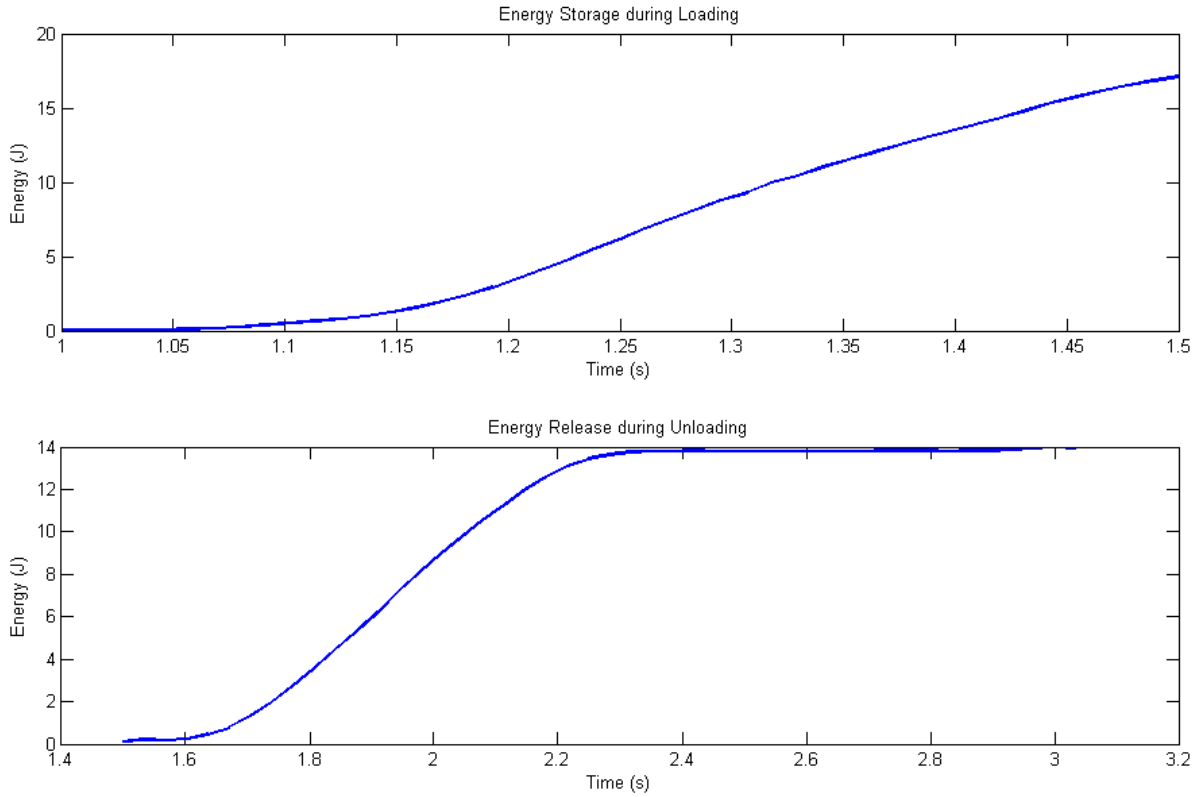


Fig. 42: The energy storage and release of the TSMLS spring.

A quick sanity check is performed by ensuring that  $E_{release} < E_{storage}$ . The spring stores 17.12 J of energy and releases 13.97 J, which gives a damping of 18.36%. These are summarized in Table X:

TABLE X: Squat test calculated forces and deformations.

Quantity	Value
$E_{storage}$ [J]	17.12
$E_{release}$ [J]	13.97
Percent Damping	18.36%

As another sanity check a very crude calculation was performed to check the percentage of energy stored that is required to perform a squat motion. Using the equation

$$W = Fd \quad (17)$$

Where  $F$  is the user's weight (800 N) and  $d$  is the distance to return to stance from squatting (0.3m), a work of 234.1 J is required. Noting that the muscular efficiency of work is 50% [25], this means 468.2 J of total metabolic work must be put in. An energy release of 13.97 J for each of the two springs corresponds to approximately *6% of the energy needed to perform a squat*. While a more elegant solution to the relationship between metabolic work of a single squat and the metabolic advantage of endurance activities is still being concocted, the fact that this is close to the average 12% augmentation achieved with the TSMLS is a good sign.

## IX. BUDGET

Creating the exoskeletons on a small budget of \$500 was important to the project since one of its main benefits is that it is meant to be a low-cost alternative to the prohibitively expensive yet much stronger active exoskeletons used in the military and for rehabilitative purposes. It is meant to be available on a manual laborer's salary.

This weighed heavily on many decisions regarding the design of the device. For example, fiberglass was chosen over carbon fiber as the spring materials because it provides similar strength and flexibility at a considerably lower cost. The thigh connections to the device were hand-formed from polycarbonate instead of purchasing a professionally made knee brace for attachment, which would have roughly doubled the price.

*The total cost for this project was \$706.95. The portion of the ES 100hf budget used was \$264.88.*

All materials were either purchased through the ES 100hf staff and McMaster-Carr or were provided by the MIT Media Lab Biomechatronics group and are displayed in Appendix A. Note that the materials provided by the MIT Media Lab are included in the total cost but not the portion of the ES 100hf budget used. It should also be noted that the dimensions of the fiberglass and aluminum stock included in the Bill were much larger than were needed or used, and stock of such large dimensions were only chosen because they had already been purchased and were in the lab. If the stock had been purchased with the considerations of this specific project in mind, the dimensions and therefore the cost would be much lower. This was also explained in the Budget section above.

Finite Element Analysis proved that the strap hinges purchased would likely be too weak for loading of the springs, so the strut hinges were purchased. These hinges were steel, giving them an advantage during cyclical loading because of the endurance limit of ferrous materials. The strap hinges were not used. Because of time considerations, design iteration including the rod ends in the boot connections were left for future work, and they were not yet used.

Furthermore, some of the aluminum used for bending into connections between springs, as well as that used in the attempt to epoxy flange pieces, was wasted as part of design process.

Taking all of this into account, an estimated cost of the actual exoskeleton device was created by multiplying stock prices, fastener package quantities, etc by the fractions actually used for the exoskeleton devices. The estimate *does* include the cost of materials provided by the MIT Media Lab but does *not* include any materials not used. This represents a more accurate cost of the device that would be used for manufacturing, and is still on the high end considering lower material costs in bulk quantities during mass production.

*The estimated device cost is at or below \$347.83.*

# X. CONCLUSION

## A. Significance

The results from the metabolic testing show that *the exoskeleton is successful at augmenting muscular endurance in lower-limb activities such as squatting, providing a significant metabolic advantage*. A comparison of design specifications to data from the results is summarized below in Table XI. The only specification not met was the requirement that the device not hinder the user while walking—because the hinge and user’s ankle are not at the same location, rotation of the ankle can be cumbersome, and walking is rather difficult. However, now that the concept of passive elastic augmentation has been solidified for lower limbs, more elegant prototypes can be constructed that take this into account.

Furthermore, the fact that this exoskeleton was created for under \$350 is a sign that the project was successful in creating a low-cost alternative to other existing exoskeleton devices.

TABLE XI: A summary of desired design specifications.

<b>Design Specification</b>	<b>Desired Value</b>	<b>Results</b>
User Weight	$\sim 800$ N	802.63 N
User Height	$\geq 1.82$ m	1.90 m
Elastic Translation	$\sim 0.3$ m	0.295 m
Effective Elastic Rotation	90°	90°
Upward Force-Weight Ratio	$\sim 0.25$	0.2526
Total Upward Force	200 N	202.72 N
Metabolic Advantage	$\geq 10\%$	11.86%
<i>Do not interfere substantially with normal gait</i>		<i>Unsuccessful</i>

## B. Future Work

The metabolic advantage of the TSMLS exoskeleton proved to be significant; however, there is still much to be done in terms of refining and improving the device to optimize its augmentation of muscular endurance and streamline its ergonomic design.

- 1) More thicknesses of fiberglass should be tested on users in terms of metabolic advantage. The passive elastic exoskeleton design at the MIT Media Lab Biomechatronics group tested six different spring stiffnesses in order to optimize their results [17]—the same can be done in the lower limbs.
- 2) In order to publish a study with the results of the exoskeleton, it must be tested on more users.
- 3) Design must be altered to better accommodate walking. This can most likely be done with the least effort at the boot hinge connection by having the hinge rotate about an axis coincident with that of the human ankle.
- 4) Design must also be altered to avoid the spring “bottoming out” during loading. Because of the nature of the boot hinge, the spring swings back and touches the ground, creating an unforeseen other grounding point and further convoluting the mechanics of spring stiffness. During testing, this

effect was negated by having the user stand on a small raised platform—however, a small tweak in the spring ankles should be able to remove this problem.

- 5) Failure testing should be done on the spring to find where and when it will break. Because of the large deformations involved, a Finite Element Analysis will likely produce inaccurate results; rather, this should be determined empirically. An academic response was already provided earlier given the data in Fig. 15, but this should be proven using actual testing. This will also demonstrate the "weakest link" of the spring, showing which component will fail first, which is important for understanding the types of likely failure modes and their relative dangers to the user. This is important in order to comply with, for example, OSHA standards.

### *C. Context*

Once the design is iterated, improved, and the augmentation of muscular endurance is optimized, the applications for the TSMLS exoskeleton device to benefit workers worldwide are broad. Any manual labor that involves these lower-limb exercises can be directly benefitted by the use of this device. Ergonomic consideration of manual labor tasks in professions such as warehouse work, construction, or the moving business can be handled by the exoskeleton instead of requiring redesign of the spaces and tasks themselves. This allows both people and businesses to be more flexible.

The implications of a passive, elastic exoskeleton to provide a substantial metabolic advantage are significant. As this concept in the lower limbs was an extension of a similar device in the upper limbs for climbing, it is reasonable to infer that this technology can likewise be extended to all the muscle groups in the human body. Indeed, one can envision more sophisticated devices that consist of combinations of such passive, elastic systems for multiple regions of the body, or an all encompassing elastic "suit" that can optimize all movements.

The time is coming where the marriage of technology and human motion can augment human ability and extend the reach of human potential. This design project and the efforts of the MIT Media Lab's Biomechatronics group represent efforts to revolutionize the way that technology interacts with the movements of the human body in order to make humans capable of achieving more than ever before in the past. Progress along this path will only continue in the years to come.

## XI. ACKNOWLEDGEMENTS

Special thanks are given to Elliott Rouse for his invaluable guidance, wealth of knowledge, unflappable patience, and good humor during the course of this project, as well as Luke Mooney for his guidance during design and prototyping phases. The cooperation of Professor Hugh Herr and the MIT Media Lab's Biomechatronics group is greatly appreciated.

Thanks are also given Dr. Daniela Faas for her support in the organization of the course, leading section, and guidance throughout the year, as well as Professor Katia Bertoldi for her assistance in the grading of this project.

Finally, thanks are given to Jordan Stephens and Peter Kjeer for their help in the machine shop and ordering parts, as well as Andreas Haggerty, Patrick Thornycroft, and Aron Zingman for their help in overcoming all logistical design and prototyping problems. The work done by the entire ES 100hf staff made this senior design project experience both rewarding and enjoyable.

## REFERENCES

- [1] K. Lawrence, "Your aching back: A look at back strain in the workplace," *Job Safety and Health Quarterly*, Fall 1990.
- [2] U. D. of Labor, "Back injuries—nation's #1 workplace safety problem," Tech. Rep. Fact Sheet No. OSHA 89-09, U.S. Department of Labor, 1990.
- [3] F. Fathallah, J. Meyers, and I. Janowitz, "Stooped and squatting postures in the workplace," in *COEH Conference Proceedings*, July 2004.
- [4] A. Gams and et al., "Effects of robotic knee exoskeleton on human energy expenditure," *IEEE Transactions on Biomedical Engineering*, vol. 60, pp. 1644–1646, June 2013.
- [5] A. Dollar and H. Herr, "Lower extremity exoskeletons and active orthoses: Challenges and state-of-the-art," *IEEE Transactions on Robotics*, vol. 24, no. 1, pp. 144–158, 2008.
- [6] N. Yagn, "Apparatus for facilitating walking, running, and jumping," 1890.
- [7] S. Zaroodny, "Bumpusher—a powered aid to locomotion," Tech. Rep. Tech. Note 1524, U.S. Army Ballistics Res. Lab, Aberdeen Proving Ground, MD, 1963.
- [8] B. Fick and J. Madison, "Hardiman i prototype for machine augmentation of human strength and endurance: Final report," Tech. Rep. GE Tech. Rep. S-71-1056, General Electric Company, Schenectady, NY, 1971.
- [9] E. Garcia, J. Sater, and J. Main, "Exoskeletons for human performance augmentation (ehpa): A program summary," *J. Robot Soc. Japan*, vol. 20, no. 8, pp. 44–48, 2002.
- [10] E. Guizzo and H. Goldstein, "The rise of the body bots," *IEEE Spectr.*, vol. 42, pp. 50–56, October 2005.
- [11] C. Walsh, K. Paresh, and H. Herr, "An autonomous, underactuated exoskeleton for load-carrying augmentation," in *in Proc. IEEE/RSJ Int. Conf. Intell. Robots Syst. (IROS)*, (Beijing, China), pp. 1410–1415, 2006.
- [12] H. Kawamoto and Y. Sankai, "Power assist system hal-3 for gait disorder person," in *in Proc. Int. Conf. Comput. Helping People Special Needs (ICCHP)(Lecture Notes on Computer Science)*, vol. 2398, (Berlin, Germany: Springer-Verlag), 2002.
- [13] K. Yamamoto, K. Hyodo, M. Ishii, and T. Matsuo, "Development of power assisting suit for assisting nurse labor," *JSME Int. J. Ser. C*, vol. 45, no. 3, pp. 703–711, 2002.
- [14] C. Walsh, K. Endo, and H. Herr, "A quasi-passive leg exoskeleton for load-carrying augmentation," *Int. J. Hum. Robot*, vol. 4, pp. 487–506, March 2007.
- [15] J. Pratt, B. Krupp, C. Morse, and S. Collins, "The roboknee: An exoskeleton for enhancing strength and endurance during walking," in *ICRA Proceedings on Robotics and Automation: 2004 Proceedings*, pp. 2430–2435, April 2004.
- [16] T. Rahman, W. Sample, S. Jayalumar, and et al., "Passive exoskeletons for assisting limb movement," *Journal of Rehabilitation Research and Development*, vol. 43, no. 5, pp. 583–590, 2006.
- [17] H. Herr and N. Langman, "Optimization of human-powered elastic mechanisms for endurance amplification," *Structural Optimization*, vol. 13, pp. 65–67, August 1996.
- [18] M. Berns, "Enhancing human metabolic economy in stair climbing via an elastic crutch mechanism," master's thesis, Dept. Mech. Eng., Massachusetts Inst. Technol., Cambridge, MA, 2011.
- [19] C. Chu and A. Chu, "Passive exoskeleton," 2009.
- [20] H. Kazerooni and et al., "Lower extremity exoskeleton," 2011.
- [21] J. Adarraga, "Exoskeleton," 2012.
- [22] P. O'Shea, "The parallel squat," *National Strength and Conditioning Association Journal*, vol. 7, February 1985.
- [23] H. P. Gavins, "Mathematical properties of stiffness matrices," Tech. Rep. course material, Duke University, Department of Civil and Environmental Engineering, December 2013.
- [24] J. M. Brockway, "Derivation of formulae used to calculate energy expenditure in man," *Human Nutrition: Clinical Nutrition*, vol. 41C, pp. 463–471, May 1987.
- [25] B. J. Whipp and K. Wasserman, "Efficiency of muscular work," *J. Appl Physiol*, vol. 26, pp. 644–648, 1969.
- [26] A. Grabowski and H. Herr, "Leg exoskeleton reduces the metabolic cost of human hopping," *Journal of Applied Physiology*, vol. 107, pp. 670–678, May 2009.
- [27] K. Gregorczyk and et al., "Effects of a lower-body exoskeleton device on metabolic cost and gait biomechanics during load carriage," *Ergonomics*, vol. 53, pp. 1264–1275, October 2010.
- [28] D. Ferris, G. Sawicki, and A. Domingo, "Powered lower limb orthoses for gait rehabilitation," *Topics in Spinal Cord Injury Rehabilitation*, vol. 11, pp. 34–49, Fall 2005.

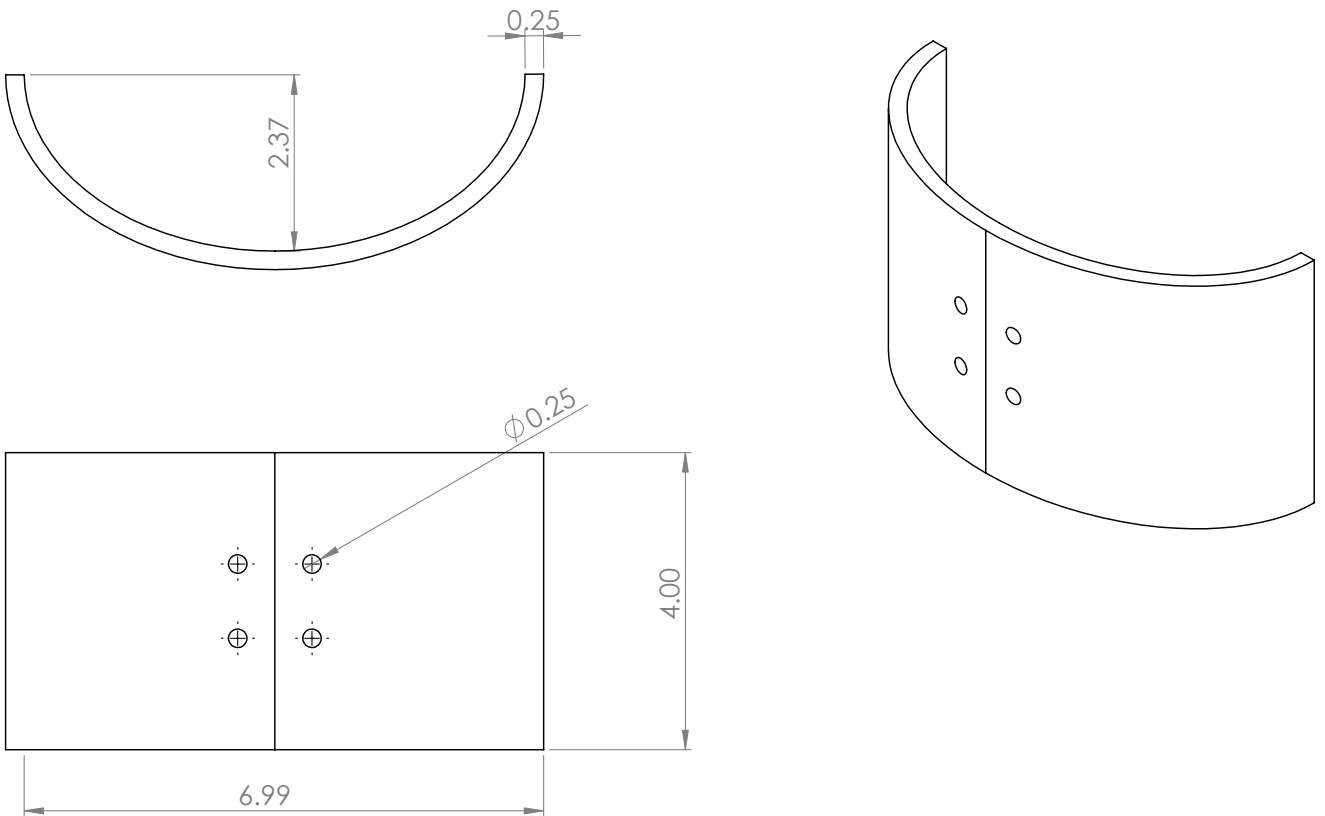
# APPENDIX A

# BILL OF MATERIALS

## APPENDIX B

### DESIGN DRAWINGS

The following pages contain the design drawings for both all the fabricated SolidWorks parts for the TSMLS exoskeleton device, as well as the purchased parts from McMaster-Carr, which functions as a specification sheet for these parts. Purchased parts with very simple dimensions (sheet stock, foam stock, straps) are not included since their dimensions are short enough to be included with their part descriptions in Appendix A.



**PROPRIETARY AND CONFIDENTIAL**  
THE INFORMATION CONTAINED IN THIS  
DRAWING IS THE SOLE PROPERTY OF  
<INSERT COMPANY NAME HERE>. ANY  
REPRODUCTION IN PART OR AS A WHOLE  
WITHOUT THE WRITTEN PERMISSION OF  
<INSERT COMPANY NAME HERE> IS  
PROHIBITED.

		UNLESS OTHERWISE SPECIFIED:				
		DIMENSIONS ARE IN INCHES TOLERANCES: FRACTIONAL $\pm$ ANGULAR: MACH $\pm$ BEND $\pm$ TWO PLACE DECIMAL $\pm$ THREE PLACE DECIMAL $\pm$	DRAWN	NAME	DATE	
			CHECKED			
			ENG APPR.			
			MFG APPR.			
		INTERPRET GEOMETRIC TOLERANCING PER:	Q.A.			
		MATERIAL	COMMENTS:			
NEXT ASSY	USED ON	FINISH				
	APPLICATION	DO NOT SCALE DRAWING				

TITLE: Thigh Connection

SIZE	DWG. NO.	REV
<b>A<thigh_piece< b=""></thigh_piece<></b>		
SCALE: 1:5	WEIGHT:	SHEET 1 OF 1

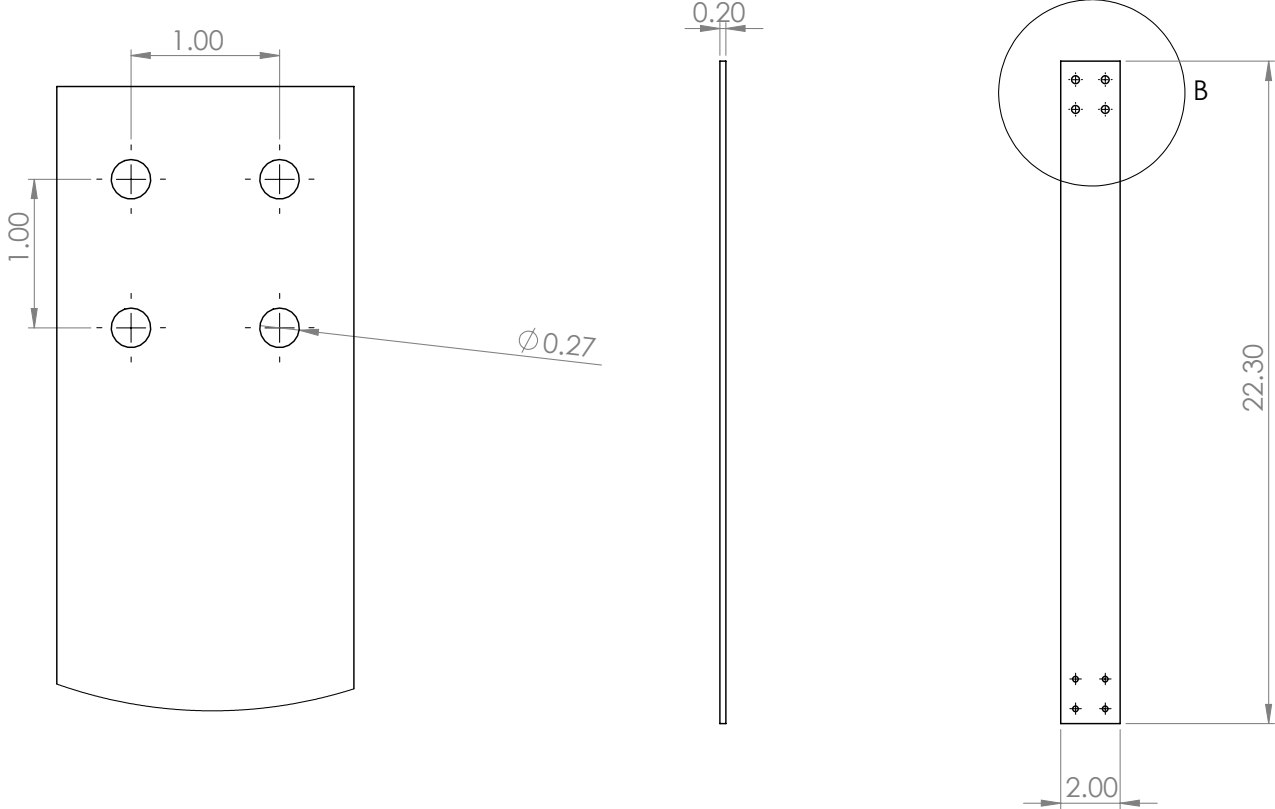
5

4

3

2

1



DETAIL B  
SCALE 1:1

**PROPRIETARY AND CONFIDENTIAL**  
THE INFORMATION CONTAINED IN THIS  
DRAWING IS THE SOLE PROPERTY OF  
<INSERT COMPANY NAME HERE>. ANY  
REPRODUCTION IN PART OR AS A WHOLE  
WITHOUT THE WRITTEN PERMISSION OF  
<INSERT COMPANY NAME HERE> IS  
PROHIBITED.

		UNLESS OTHERWISE SPECIFIED:  DIMENSIONS ARE IN INCHES TOLERANCES: FRACTIONAL ± ANGULAR: MACH. ± BEND ± TWO PLACE DECIMAL ± THREE PLACE DECIMAL ±  INTERPRET GEOMETRIC TOLERANCING PER:	DRAWN	NAME	DATE	TITLE:  <b>Spring 1</b>
		MATERIAL	CHECKED	ENG APPR.	MFG APPR.	
	NEXT ASSY	USED ON	Q.A.			COMMENTS:
	APPLICATION	FINISH				
		DO NOT SCALE DRAWING				
SIZE	DWG. NO.					REV
<b>A</b>	spring1					
SCALE: 1:5	WEIGHT:					SHEET 1 OF 1

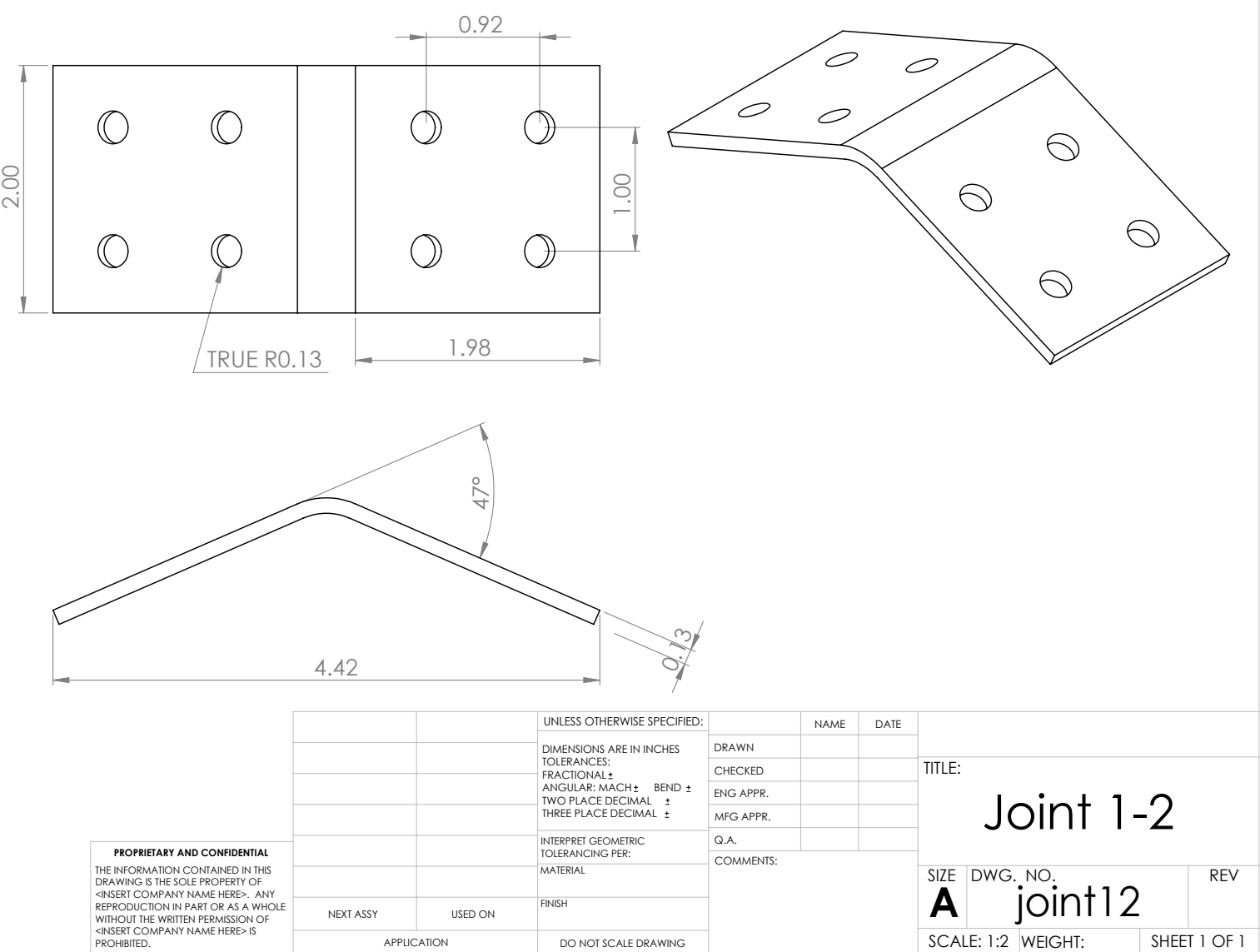
5

4

3

2

1



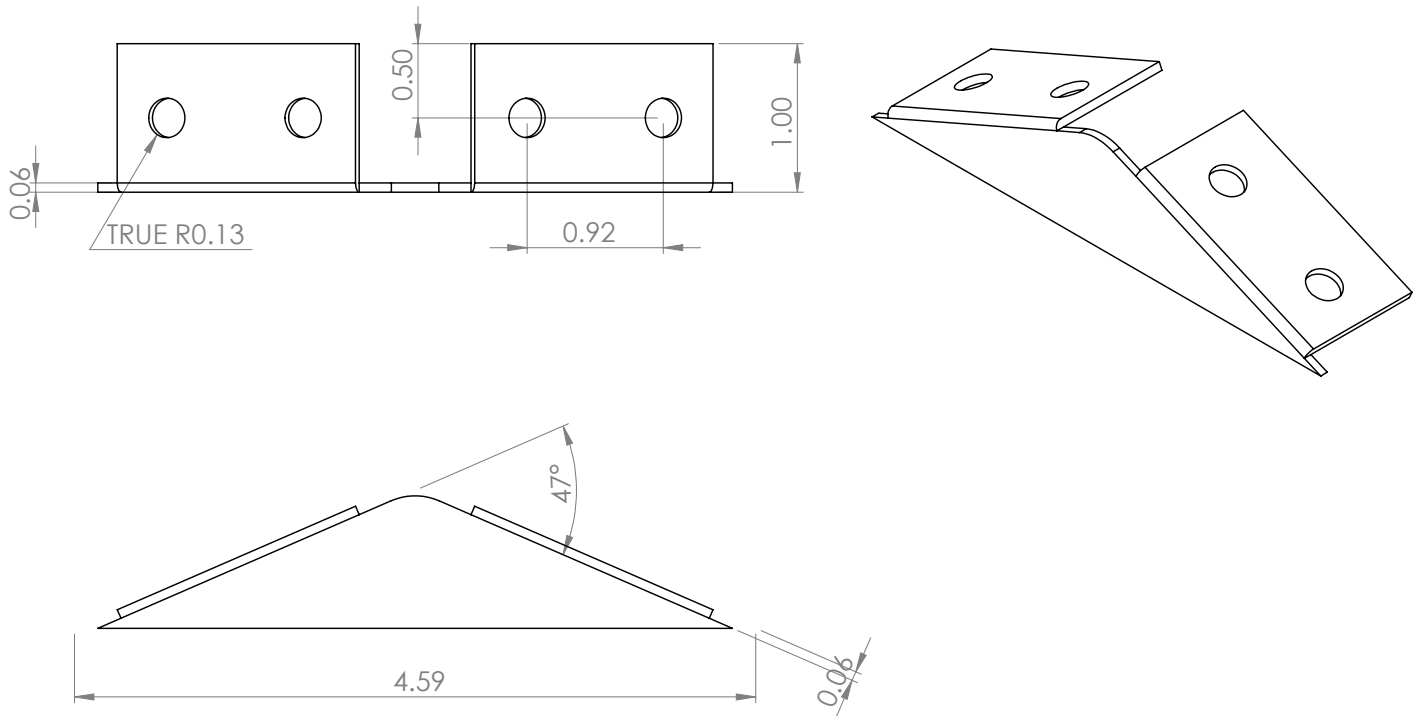
5

4

3

2

1



<b>PROPRIETARY AND CONFIDENTIAL</b> THE INFORMATION CONTAINED IN THIS DRAWING IS THE SOLE PROPERTY OF <INSERT COMPANY NAME HERE>. ANY REPRODUCTION IN PART OR AS A WHOLE WITHOUT THE WRITTEN PERMISSION OF <INSERT COMPANY NAME HERE> IS PROHIBITED.	UNLESS OTHERWISE SPECIFIED:		DRAWN CHECKED ENG APPR. MFG APPR. Q.A. COMMENTS:	NAME DATE  TITLE: <b>Flange 1-2</b>  SIZE   DWG. NO. <b>A</b> flange12   REV		
	DIMENSIONS ARE IN INCHES					
	TOLERANCES:					
	FRACTIONAL $\pm$					
	ANGULAR: MACH $\pm$ BEND $\pm$					
	TWO PLACE DECIMAL $\pm$					
	THREE PLACE DECIMAL $\pm$					
INTERPRET GEOMETRIC TOLERANCING PER:						
MATERIAL						
NEXT ASSY						
USED ON						
FINISH						
APPLICATION		DO NOT SCALE DRAWING				

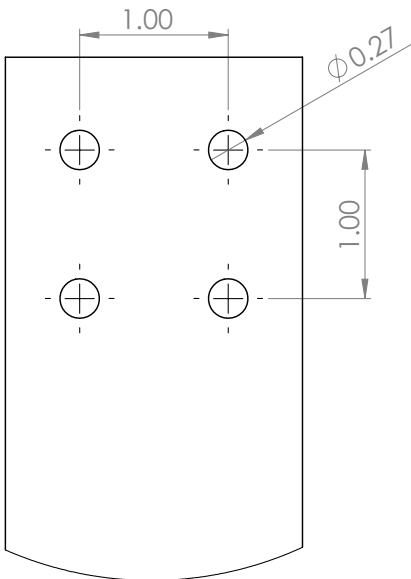
5

4

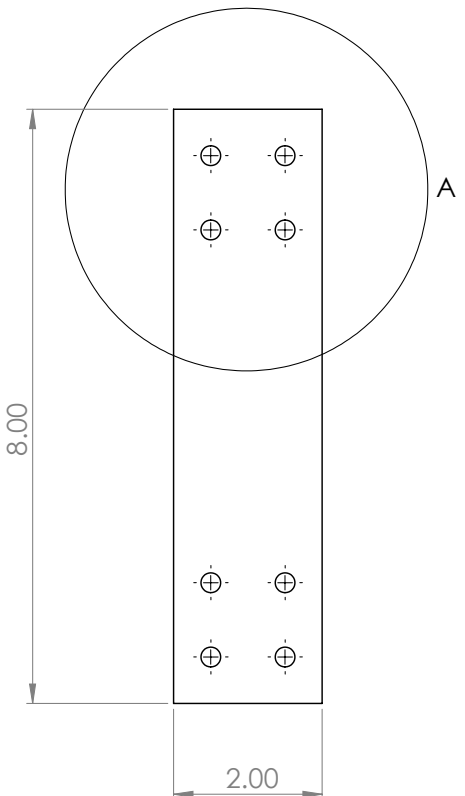
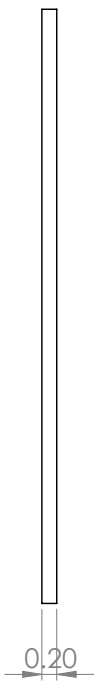
3

2

1



DETAIL A  
SCALE 1:1



**PROPRIETARY AND CONFIDENTIAL**  
THE INFORMATION CONTAINED IN THIS  
DRAWING IS THE SOLE PROPERTY OF  
<INSERT COMPANY NAME HERE>. ANY  
REPRODUCTION IN PART OR AS A WHOLE  
WITHOUT THE WRITTEN PERMISSION OF  
<INSERT COMPANY NAME HERE> IS  
PROHIBITED.

		UNLESS OTHERWISE SPECIFIED:  DIMENSIONS ARE IN INCHES TOLERANCES: FRACTIONAL ± ANGULAR: MACH ± BEND ± TWO PLACE DECIMAL ± THREE PLACE DECIMAL ±  INTERPRET GEOMETRIC TOLERANCING PER:  MATERIAL	DRAWN	NAME	DATE	TITLE:  <b>Spring 1</b>
			CHECKED			
			ENG APPR.			
			MFG APPR.			
		NEXT ASSY	USED ON	FINISH	COMMENTS:	
		APPLICATION		DO NOT SCALE DRAWING		
						SIZE DWG. NO. <b>A</b> <b>spring2</b> REV
						SCALE: 1:2 WEIGHT: SHEET 1 OF 1

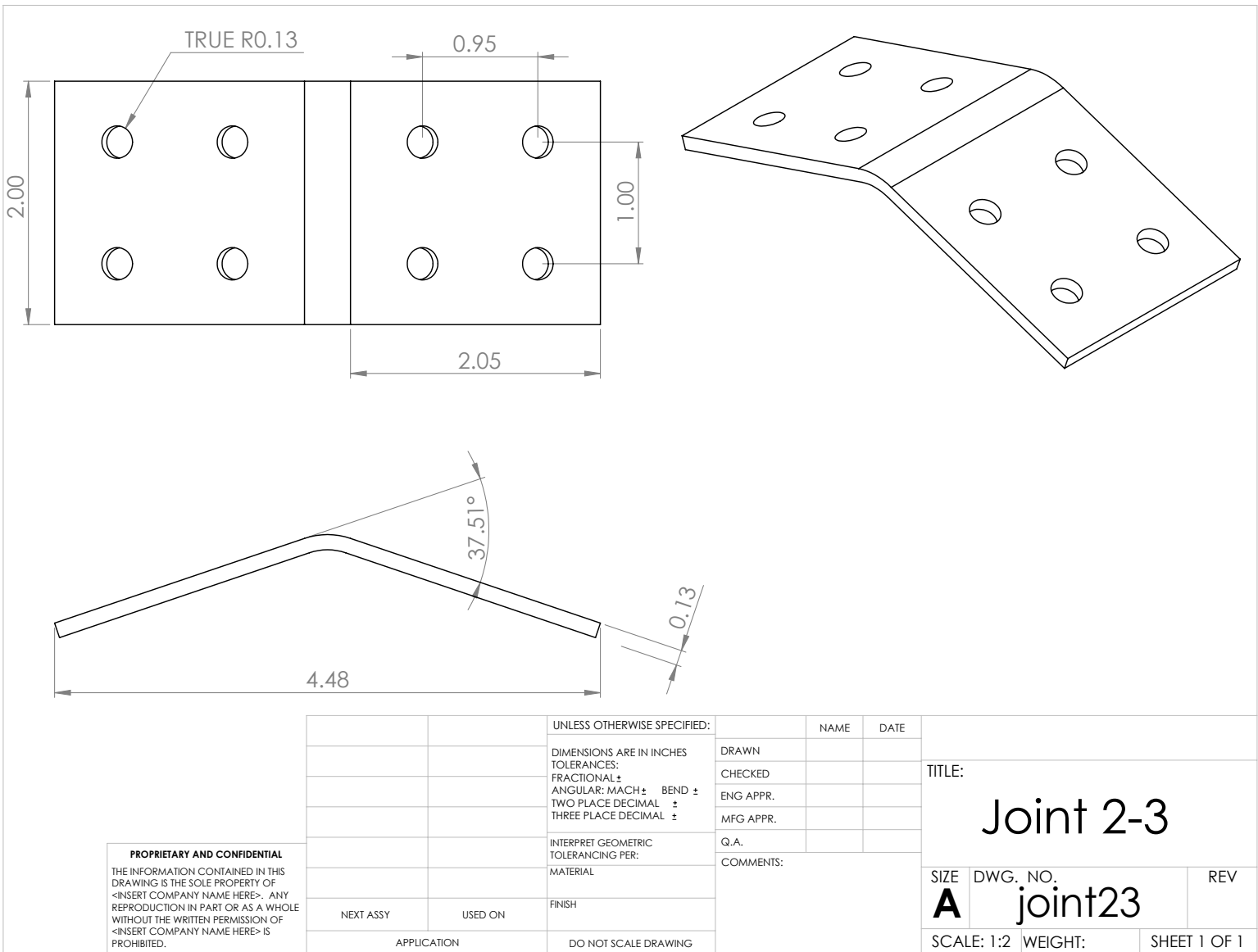
5

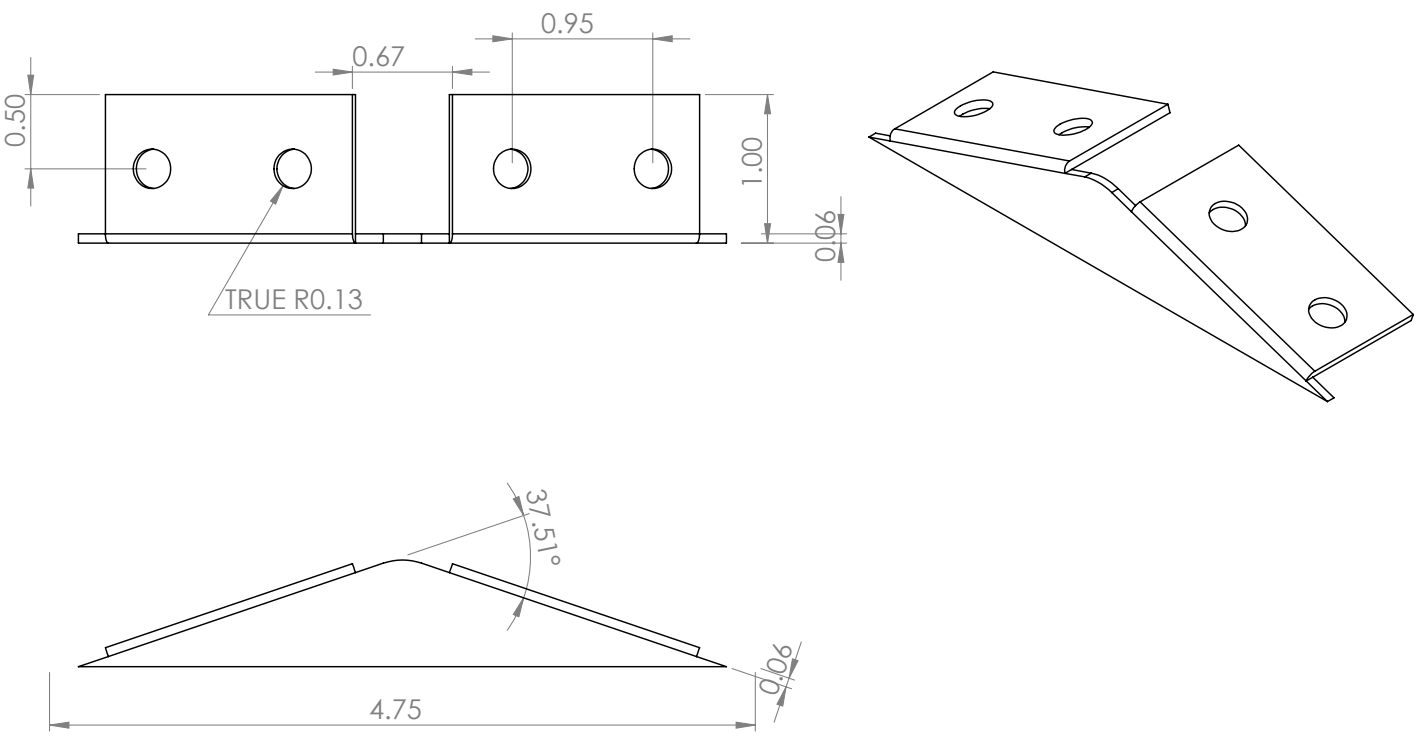
4

3

2

1

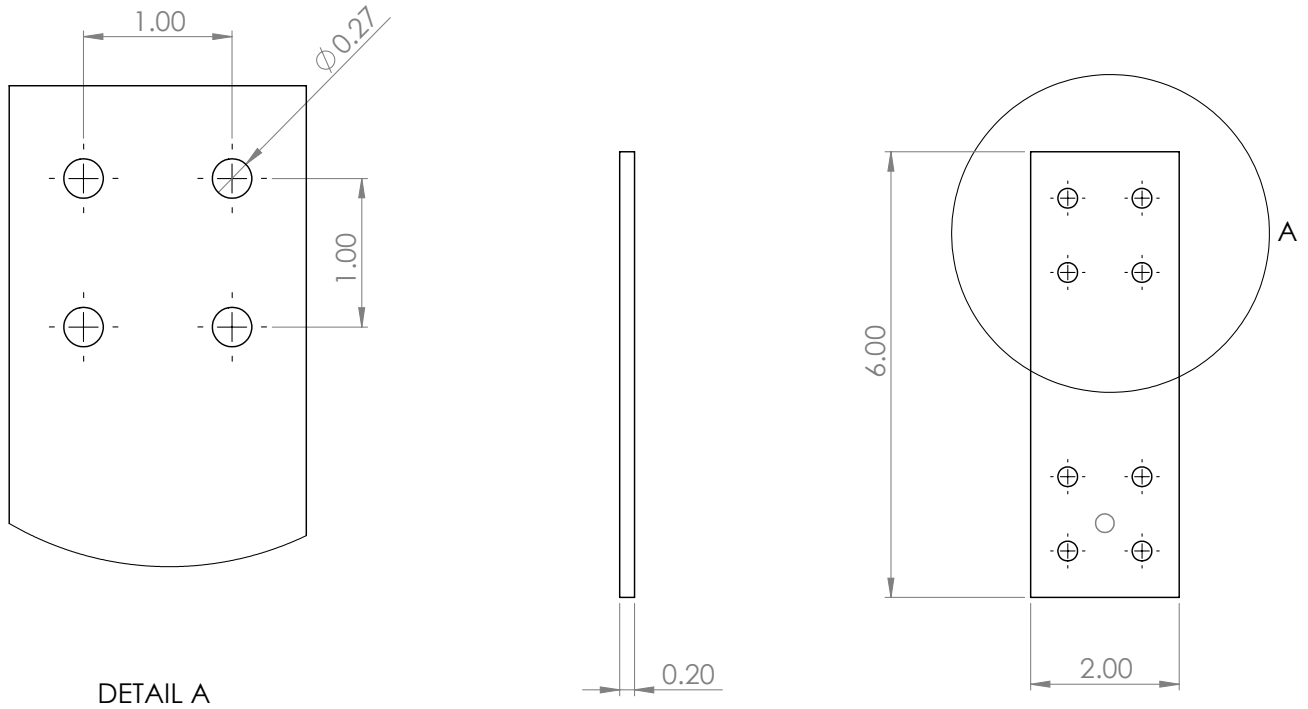




		UNLESS OTHERWISE SPECIFIED:		NAME	DATE	TITLE:  <b>Flange 2-3</b>
		DIMENSIONS ARE IN INCHES	DRAWN			
		TOLERANCES:	CHECKED			
		FRACTIONAL ±	ENG APPR.			
		ANGULAR: MACH ± BEND ±	MFG APPR.			
		TWO PLACE DECIMAL ± THREE PLACE DECIMAL ±	Q.A.			
		INTERPRET GEOMETRIC TOLERANCING PER:	COMMENTS:			
		MATERIAL				
NEXT ASSY	USED ON	FINISH				SIZE    DWG. NO. <b>A flange23</b>
APPLICATION		DO NOT SCALE DRAWING				
			SCALE: 1:2	WEIGHT:	SHEET 1 OF 1	

**PROPRIETARY AND CONFIDENTIAL**

THE INFORMATION CONTAINED IN THIS DRAWING IS THE SOLE PROPERTY OF <INSERT COMPANY NAME HERE>. ANY REPRODUCTION IN PART OR AS A WHOLE WITHOUT THE WRITTEN PERMISSION OF <INSERT COMPANY NAME HERE> IS PROHIBITED.



DETAIL A  
SCALE 1 : 1

**PROPRIETARY AND CONFIDENTIAL**  
THE INFORMATION CONTAINED IN THIS  
DRAWING IS THE SOLE PROPERTY OF  
<INSERT COMPANY NAME HERE>. ANY  
REPRODUCTION IN PART OR AS A WHOLE  
WITHOUT THE WRITTEN PERMISSION OF  
<INSERT COMPANY NAME HERE> IS  
PROHIBITED.

		UNLESS OTHERWISE SPECIFIED:  DIMENSIONS ARE IN INCHES TOLERANCES: FRACTIONAL ± ANGULAR: MACH ± BEND ± TWO PLACE DECIMAL ± THREE PLACE DECIMAL ±	DRAWN	NAME	DATE	TITLE:  <b>Spring 3</b>
		INTERPRET GEOMETRIC TOLERANCING PER:	CHECKED			
		MATERIAL	ENG APPR.			
			MFG APPR.			
			Q.A.			
		COMMENTS:				
NEXT ASSY	USED ON	FINISH				SIZE DWG. NO. <b>A</b> <b>spring3</b> REV
APPLICATION		DO NOT SCALE DRAWING				SCALE: 1:2 WEIGHT: SHEET 1 OF 1

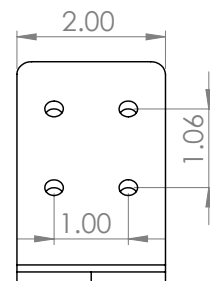
5

4

3

2

1



		UNLESS OTHERWISE SPECIFIED:		NAME	DATE	
		DIMENSIONS ARE IN INCHES TOLERANCES: FRACTIONAL $\pm$ ANGULAR: MACH $\pm$ BEND $\pm$ TWO PLACE DECIMAL $\pm$ THREE PLACE DECIMAL $\pm$	DRAWN			
			CHECKED			TITLE:
			ENG APPR.			
			MFG APPR.			
		INTERPRET GEOMETRIC TOLERANCING PER:	Q.A.			
		MATERIAL	COMMENTS:			
NEXT ASSY	USED ON	FINISH				
	APPLICATION	DO NOT SCALE DRAWING				
SIZE	DWG. NO.					REV
	Aboot_connect					
SCALE: 1:2	WEIGHT:					SHEET 1 OF 1

**PROPRIETARY AND CONFIDENTIAL**  
THE INFORMATION CONTAINED IN THIS  
DRAWING IS THE SOLE PROPERTY OF  
<INSERT COMPANY NAME HERE>. ANY  
REPRODUCTION IN PART OR AS A WHOLE  
WITHOUT THE WRITTEN PERMISSION OF  
<INSERT COMPANY NAME HERE> IS  
PROHIBITED.

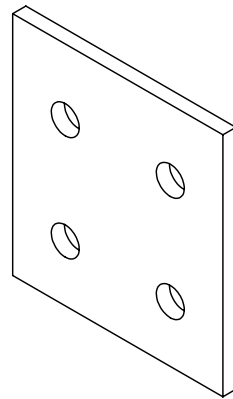
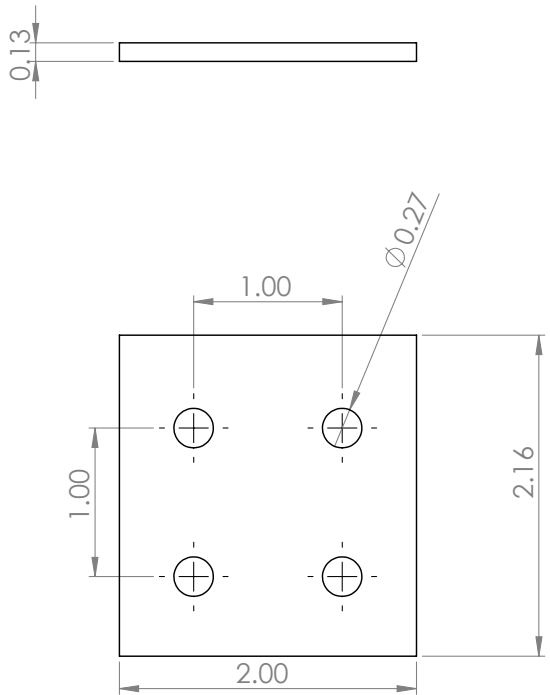
5

4

3

2

1



		UNLESS OTHERWISE SPECIFIED:		NAME	DATE	
		DIMENSIONS ARE IN INCHES	DRAWN			
		TOLERANCES:	CHECKED			
		FRACTIONAL $\pm$	ENG APPR.			
		ANGULAR: MACH $\pm$ BEND $\pm$	MFG APPR.			
		TWO PLACE DECIMAL $\pm$	Q.A.			
		THREE PLACE DECIMAL $\pm$	COMMENTS:			
		INTERPRET GEOMETRIC TOLERANCING PER:				
		MATERIAL				
	NEXT ASSY	USED ON				
		APPLICATION	DO NOT SCALE DRAWING			

**PROPRIETARY AND CONFIDENTIAL**  
THE INFORMATION CONTAINED IN THIS  
DRAWING IS THE SOLE PROPERTY OF  
<INSERT COMPANY NAME HERE>. ANY  
REPRODUCTION IN PART OR AS A WHOLE  
WITHOUT THE WRITTEN PERMISSION OF  
<INSERT COMPANY NAME HERE> IS  
PROHIBITED.

TITLE: **Pressure Plate**  
SIZE **A** DWG. NO. **pressure plate** REV **V**  
SCALE: 1:1 WEIGHT: **1** SHEET 1 OF 1

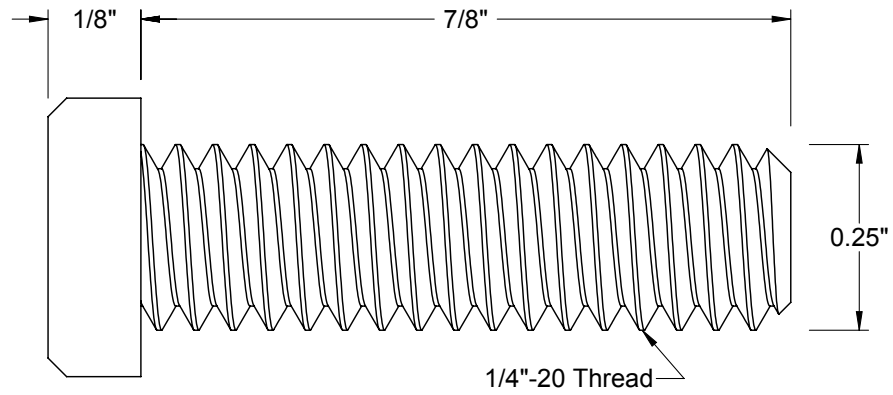
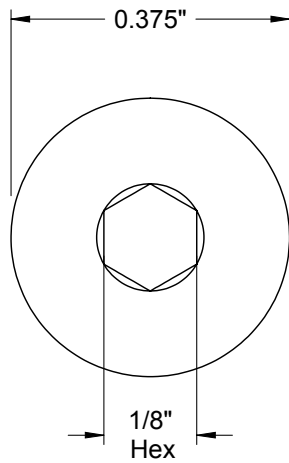
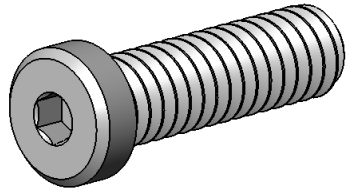
5

4

3

2

1



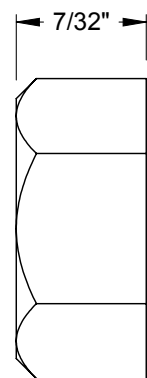
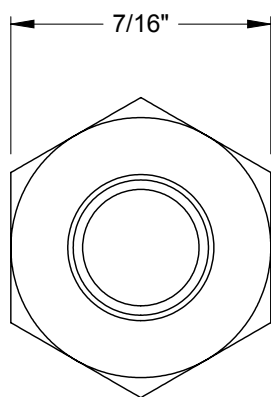
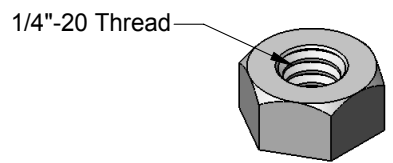
**McMASTER-CARR** CAD

<http://www.mcmaster.com>  
© 2013 McMaster-Carr Supply Company

Information in this drawing is provided for reference only.

PART  
NUMBER **92220A204**

Low-Profile Alloy Steel  
Socket Head Cap Screw



**McMASTER-CARR** CAD

<http://www.mcmaster.com>

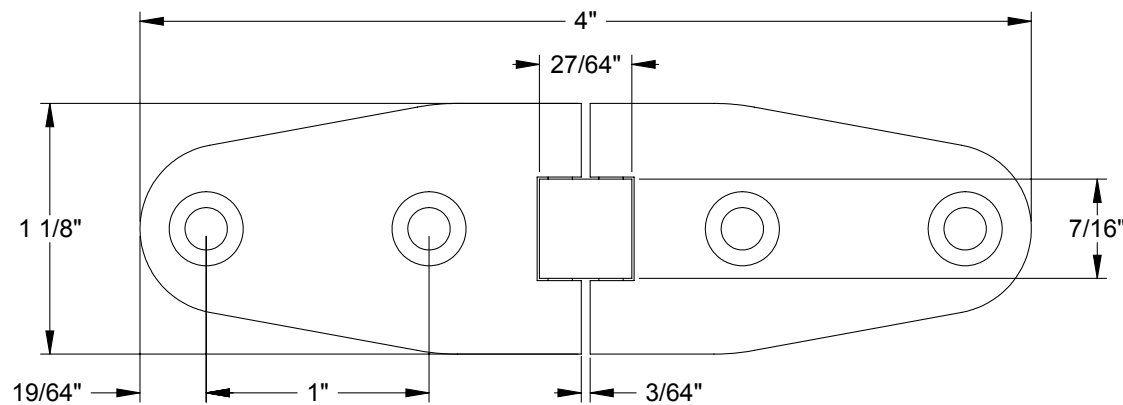
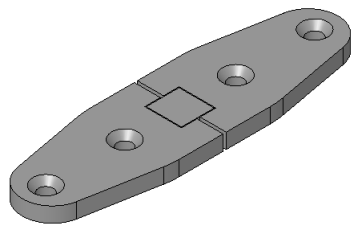
© 2009 McMaster-Carr Supply Company

Information in this drawing is provided for reference only.

PART  
NUMBER

**95479A111**

Black Oxide Grade 5 Steel  
Hex Nut



Hinge uses #10 flat head screws.

**McMASTER-CARR** CAD

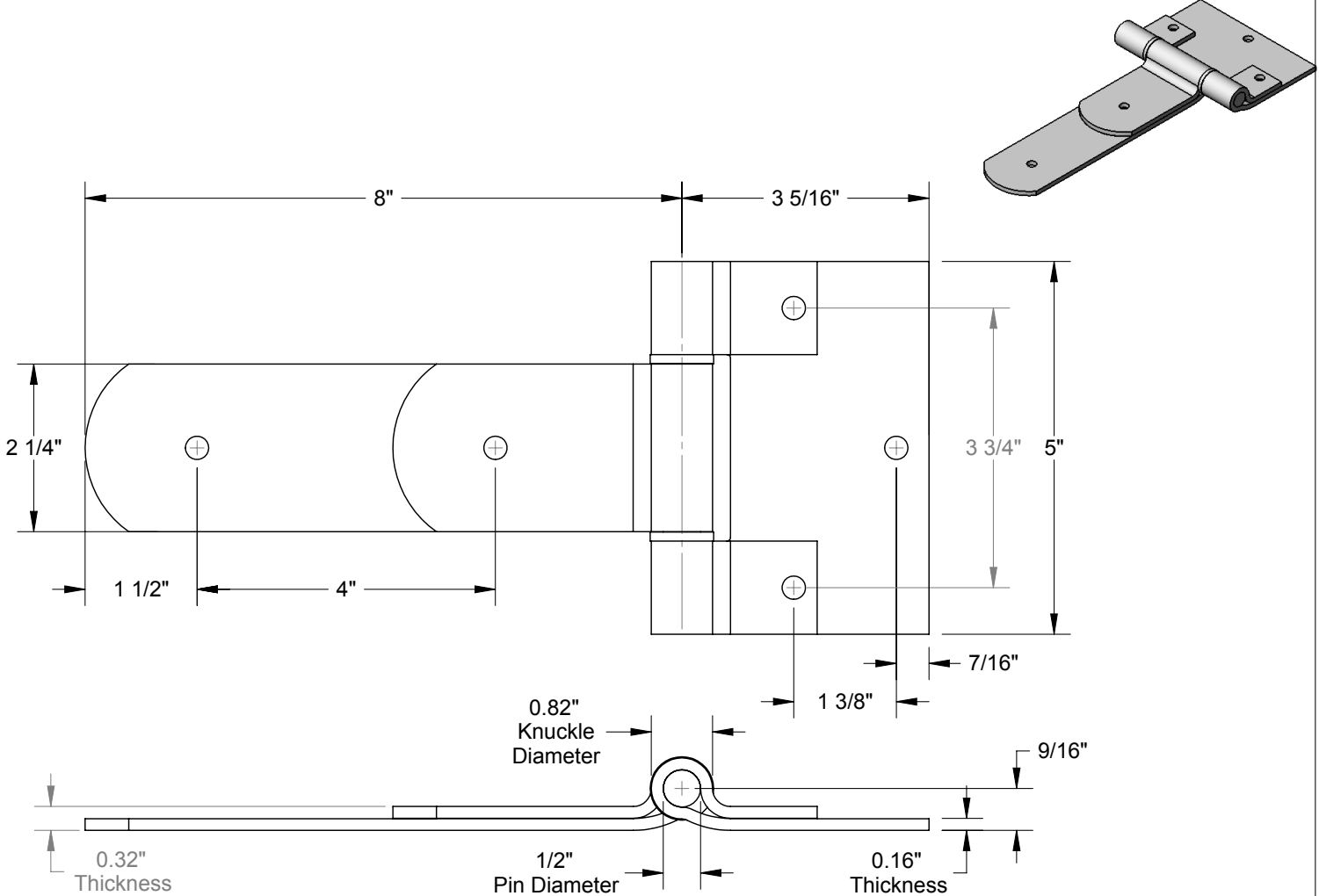
<http://www.mcmaster.com>  
© 2013 McMaster-Carr Supply Company

Information in this drawing is provided for reference only.

PART  
NUMBER

**1528A27**

Strap  
Hinge



Hinge uses 5/16" screws.

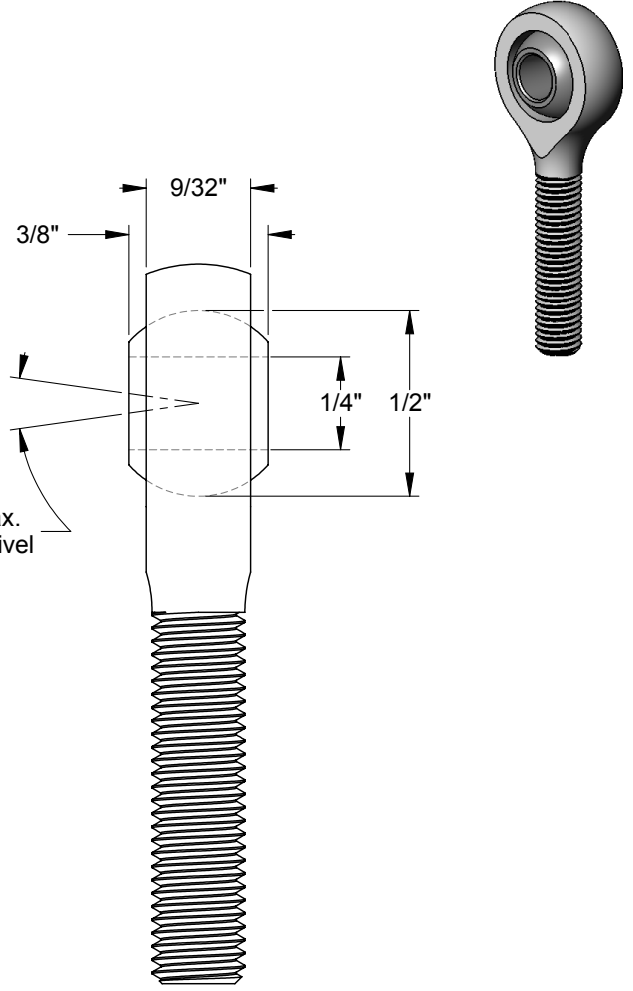
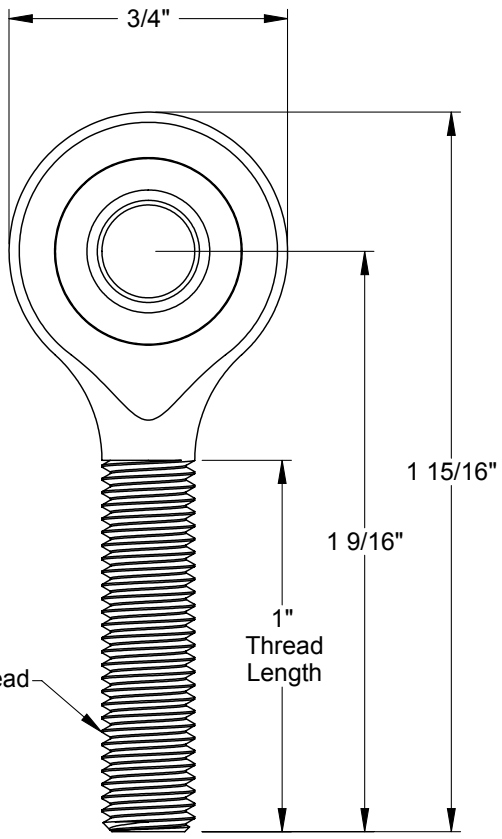
**McMASTER-CARR** CAD

<http://www.mcmaster.com>  
© 2013 McMaster-Carr Supply Company  
Information in this drawing is provided for reference only.

PART  
NUMBER

**350T12**

Strut  
Hinge



Notes:

Zinc-Plated Chrome-Alloy Steel Housing with Chrome-Plated Bearing Steel Ball and PTFE-Lined Steel Insert

**McMASTER-CARR** CAD

<http://www.mcmaster.com>  
© 2012 McMaster-Carr Supply Company  
Information in this drawing is provided for reference only.

PART  
NUMBER

**60745K221**

Right-Hand Thread  
Ball Joint Rod End

# APPENDIX C

## MATLAB CODE

### A. Exo Video Processing

This is a MATLAB script, *exo\_video\_processing.m*, that reads a video file and utilizes functions from the computer vision toolkit to give deformation data and angle of applied force.

After initializing some empty vectors to contain all the data, the script opens a video reader, video player, and video writer object. The ellipsedata was actually gathered by running this script a previous time, running that through *stiffness\_matrix.m*, and bring that data back again. A point tracker, a *detectHarrisFeatures* object, is initialized and trained on notable points of the first frame.

This script iterates through each frame of the video data and refreshes the point tracker to track the motion of notable points. The point indices of the thigh connection of the spring, as well as the force sensor, were found by searching the pixel coordinates of the desired points. Markers were placed on these point indices, and a vector was drawn between the thigh and sensor to find the angle of applied force. The first frame's thigh location was taken to be the origin of the coordinate system.

Once the deformations started at frame 37, vectors of the ellipse major and minor axes were plotted using the *quiver* and *getframe* commands, as well as the ellipses themselves. At every frame, the video writer object writes that frame to a new video file. After all the frames have been analyzed, the video reader, player, and writer objects are released.

```

% exo_video_processing.m: Loads in video data, trains object tracker to
% track spring deformation as well as direction of force. Loads in force
% data from stiffness testing, creates vectors of force magnitude, spring
% deformation, and force direction. Coordinate system defined as original
% tracked spring position as (0,0) and angle of longest spring as x-axis.
%
% Nicolas Hite
% 01/25/14
% ES 100hf
%o
% Info: calipers are set to five inches. = 133 px, measured with imtool()
% -> ratio is 133/5 = 26.6 px/in
clear, close all

% Define some things.
px2in = 26.6;           % pixel-to-inch ratio.
springLocs = [];         % spring corner location per frame (in px)
unshiftedXandY = [];% Unshifted x and y. Duh.
deformations = [];% deformation of spring from zeroZero in inches
deformationXandY = [];% shifted x and y. Pretty self-explanatory.
zeroZero = [];% initial spring location from firstFrame
xAxis = [];% reference line to compare to force vectors
forceVectors = [];% direction of force
forceAngles = [];% directions of applied forces
isFirst = true;% check if it's first frame to initialize zeroZero
trails = [];

% Load movie and define player and writer.
VideoFReader = vision.VideoFileReader('Exo_characterization_test_1.avi');
VideoPlayer = vision.VideoPlayer;
vidWriter = VideoWriter('Exo_test_1_ellipses.avi');
open(vidWriter);

ellipsedata = load('ellipsedata.mat');

forceXY1 = ellipsedata.forceXY1;
defXY1 = ellipsedata.defXY1;
Bs1_filt = ellipsedata.Bs1_filt;
n = length(defXY1(:,1)) -1;

% Define point tracker, set tolerance.
PointTracker = vision.PointTracker('MaxBidirectionalError', 10);

% Initialize and train PointTracker from first frame point data.
firstFrame = step(VideoFReader);
points = detectHarrisFeatures(rgb2gray(firstFrame));
initialize(PointTracker, points.Location, firstFrame);

% Load Test 1 data.
test1Data = load('test1.mat');
plot(test1Data.ftime,test1Data.force)
% Play video and grab tracking data.
for j = 1:(length(Bs1_filt) + 36)

    % Grab points from interated frame.
    frame = step(VideoFReader);
    [points, validity] = step(PointTracker, frame);

```

```

% Using imtool we find px location of points of interest.
% Find which points they are by searching via location.
% Spring is 303, sensor is 287, axis is 141
springIndex = 303;
sensorIndex = 287;
axisIndex = 141;
specialPoints = [points(sensorIndex,:); points(springIndex,:)];

% Make markers and line in video.
%out = insertMarker(frame,points,'+');
specialOut = insertMarker(frame,
[specialPoints(1:2);specialPoints(3:4)],'+','Size',5,'Color','red');
specialOut =
insertShape(specialOut,'Line',specialPoints,'Color','green','Opacity',1);

% Store info.
% Set (0,0) location for coordinate system and x-axis
if(isFirst)
    zeroZero = specialPoints(3:4);
    xAxis = [points(axisIndex,:); specialPoints(3:4)];
    axisAngle = atand((xAxis(2) - xAxis(4))/(xAxis(3)-xAxis(1))) - 90;
    isFirst = false;
end
specialOut = insertMarker(specialOut,zeroZero,'x','Size',5,'Color','blue');
specialOut = insertShape(specialOut,'Line',xAxis,'Color','blue','Opacity',1);
% Store locations and deformations.
springLocs = [springLocs; specialPoints(3:4)]; % spring location
forceVectors = [forceVectors; specialPoints]; % force vectors
unshiftedXandY = [unshiftedXandY; (specialPoints(3:4)-zeroZero)/px2in]; % x
and y components of deformation (inches)
deformations = [deformations; sqrt(unshiftedXandY(end,1)^2 +
unshiftedXandY(end,2)^2)]; % deformations

% Calculate angle of force.
% Correct for ambiguous tan in third and second quadrants.
riseRun = atan((forceVectors(end,4) - forceVectors(end,2))/
(forceVectors(end,1)-forceVectors(end,3))/pi*180;
    if((forceVectors(end,4)-forceVectors(end,2) < 0) &&(forceVectors(end,1)-
forceVectors(end,3) < 0));
        riseRun = riseRun - 180;
    elseif((forceVectors(end,4)-forceVectors(end,2) > 0) &&(forceVectors(end,1)-
forceVectors(end,3) < 0));
        riseRun = riseRun + 180;
    end

% Make sure angles go from 0 to 180 and 0 to -180.
newAngle = riseRun - axisAngle;
if(newAngle > 180)
    newAngle = newAngle - 360;
end

forceAngles = [forceAngles; -newAngle];

% Shift coordinate system.
defAngle = atand(unshiftedXandY(end,2)/unshiftedXandY(end,1));
if(unshiftedXandY(end,2) > 0 && unshiftedXandY(end,1) < 0)
    defAngle = defAngle + 180;
end
shiftedAngle = defAngle + axisAngle;

```

```

%shiftedAngle = defAngle;
x = deformations(end)*cosd(shiftedAngle);
y = deformations(end)*sind(shiftedAngle);
deformationXandY = [deformationXandY; x y];

specialOut = insertMarker(specialOut,points,'+');
% Display frame and write to new file.
%step(VideoPlayer, specialOut);
%writeVideo(vidWriter, specialOut);

if(j < 37)
    imshow(specialOut);
else
    close all;
    imshow(frame);
    hold on;
    i = j - 36;
    K = [Bs1_filt(1,i) Bs1_filt(2,i); Bs1_filt(2,i) Bs1_filt(3,i)];
% K = [Bs1(1,i) Bs1(2,i); Bs1(2,i) Bs1(3,i)];
[V(:,:,i) D(:,:,:,i)] = eig(K);
if D(:,:,:,i) < 0
    continue
end

newdefx = zeroZero(1)+(defXY1(i,1)*px2in);
newdefy = zeroZero(2)-(defXY1(i,2)*px2in);

trails = [trails; newdefx,newdefy];
h5 = plot(trails(:,1), trails(:,2), '.', 'Color', [.8 .8 .8]);
h1 = plot(newdefx,newdefy,'ko', 'linewidth',2, 'markersize',8);
h2 = quiver(newdefx,newdefy,forceXY1(i,1)*px2in/20,-
forceXY1(i,2)*px2in/20,'g', 'linewidth',2);
h3 = quiver(newdefx,newdefy,D(1,1,i)*V(1,1,i)*px2in/10,
-D(1,1,i)*V(2,1,i)*px2in/10,'r', 'linewidth',2);
h4 = quiver(newdefx,newdefy,D(2,2,i)*V(1,2,i)*px2in/10,
-D(2,2,i)*V(2,2,i)*px2in/10,'c', 'linewidth',2);
h6 = ellipse(sqrt((D(1,1,i)*V(1,1,i)*px2in/10)^2 +
(D(1,1,i)*V(2,1,i)*px2in/10)^2),sqrt((D(2,2,i)*V(1,2,i)*px2in/10)^2 +
(D(2,2,i)*V(2,2,i)*px2in/10)^2),-atan((D(1,1,i)*V(2,1,i)/10)/
(D(1,1,i)*V(1,1,i)/10)),newdefx,newdefy,'r',3000);

frame = getframe;
writeVideo(vidWriter,frame);
%step(VideoPlayer,frame);

end
end

% Release Reader and Player objects.
release(VideoFReader);
release(VideoPlayer);
close(vidWriter);

%save ExoTrackingTest1shifted.mat deformationXandY forceAngles deformations
%%
clear, close all

```

## B. Stiffness Matrix Calculations

This is a MATLAB script that takes the force and deformation data from the previous script and uses those to perform a least-squares statistical analysis and acquire the stiffness matrices for each frame of data.

Three points a, b, and c are taken as a local and two reference points. The local points b are simply iterated through the data, and the reference points a and c are chosen by picking any point that has some  $x$  or  $y$  deformation, respectively, that is just above a chosen threshold value to ensure close proximity. For each group of points, the difference in deformation *from* local point b to each reference points are taken and reshaped into the deformation matrix  $X$ . The reaction forces *to* point b are reshaped into matrix  $Y$ . The values for each stiffness estimator  $\beta$  are computed via matrix division.

This data is noisy, so some smoothing is necessary to make it usable. First, any values that are too large (over 200) are thrown out. Second, the data is put through the *lowfilt* function to smooth it. The quiver plots are for visualizing each system of three points to make sure they are close enough and that each pair of deformation vectors is linearly independent.

Finally, these data are saved in the MATLAB data file *ellipsedata.mat* to be plugged back into *exo\_video\_processing.m*.

```

% stiffness_matrix.m: Pulls in (x,y) force and (x,y) deformation
% data obtained from exo_video_processing.m and performs the necessary
% least-squares analysis to obtain a symmetric, two-dimensional stiffness
% matrix that fully characterizes the major and minor axes of the exo's
% spring stiffness, as well as the angle of the ellipse it forms.
%
% Nicolas Hite
% 01/29/14
% ES 100hf

clear, close all;

% Load in the data.
test1Vid = load('ExoTrackingTest1shifted.mat');
test2Vid = load('ExoTrackingTest2shifted.mat');
load('test1Resampled.mat');
load('test2Resampled.mat');
ds = 1;    %desampling factor
%%
% Match up first test.
% Frame ~36 is first impulse. (force sample 740)
% Frame ~1635 is second impulse (force sample 14091)

%Snag relevant data between impulses.
defXY1(:,1) = test1Vid.deformationXandY(36:ds:1635,1); % make x deformation
positive
defXY1(:,2) = -test1Vid.deformationXandY(36:ds:1635,2); % y coordinate increased
in pixels going down frame; needn't change
angles1 = test1Vid.forceAngles(36:ds:1635);

%Number of iterations for looping through data.
n = length(defXY1(:,1)) -1;

%Construct matrices to be filled in later.
forceMatrix1 = zeros(4,n-1);      % matrix of delta f
defMatrix1 = zeros(4,3,n-1);      % matrix of delta x
Beta1 = zeros(2,2,n-1);          % 2*2 beta matrix
Bs1 = zeros(3,n-1);              % unchanged beta column to test X*B = Y

%Grab x and y components of force.
%plot(test1Data.force)
test1Data.force = test1Data.force - min(test1Data.force);    % correct for offset
forceXY1(:,1) = test1Data.force(1:ds:end).*cosd(angles1);   % make x force positive
forceXY1(:,2) = -test1Data.force(1:ds:end).*sind(angles1);

%Get stiffness matrix for each sample.

% Take a point.
for i = 2:n

    %(i-1) = point a
    % i   = point b
    %(i+1) = point c

    % Find a point whose x-component diff with i is just over .1.
    xdiff = abs(defXY1(:,1)-defXY1(i,1));
    xdiff_inx = find(xdiff > .1);
    [xmin xinx] = min(xdiff(xdiff_inx));% + .01*abs(i-[1:length(xdiff_inx)]'));

```

```

x_pt_loc = xdiff_inx(xinx);

% Find a point whose y-component diff with i is just over .5.
ydiff = abs(defXY1(:,2)-defXY1(i,2));
ydiff_inx = find(ydiff > .5);
[ymin yinx] = min(ydiff(ydiff_inx));% + .01*abs(i-[1:length(ydiff_inx)]'));
y_pt_loc = ydiff_inx(yinx);

Fxab = forceXY1(x_pt_loc,1) - forceXY1(i,1); %
Fyab = forceXY1(x_pt_loc,2) - forceXY1(i,2); %
Fxbc = forceXY1(y_pt_loc,1) - forceXY1(i,1); %
Fybc = forceXY1(y_pt_loc,2) - forceXY1(i,2); %

% Populate force matrix with each vector.
Y = [Fxab; Fyab; Fxbc; Fybc];
forceMatrix1(:,i-1) = Y;

% Define quantities for displacement vector.
Xab = -(defXY1(x_pt_loc,1) - defXY1(i,1)); %
Yab = -(defXY1(x_pt_loc,2) - defXY1(i,2)); %
Xbc = -(defXY1(y_pt_loc,1) - defXY1(i,1)); %
Ybc = -(defXY1(y_pt_loc,2) - defXY1(i,2)); %

X = [Xab Yab 0;    % for each eqn., Fxab = Kxx(Xab) + Kth(Yab + Xab) + Kyy(Yab)
      0 Xab Yab;
      Xbc Ybc 0;
      0 Xbc Ybc];

% Populate matrix of deformation matrices (3D)
defMatrix1(:,:,:,i-1) = X;

% Populate Beta matrix with least-squares regression.
B = (X'*X)\(X'*Y); % MATLAB suggested I use this instead of inv(X'*X)*X'*Y
if abs(mean(B)) > 200
    Bs1(:,i-1) = [0;0;0];
else
    Bs1(:,i-1) = B;
end

%Reshape Beta column into 2*2 (3D)
Beta1(1,1,i-1) = B(1,1);
Beta1(2,1,i-1) = B(2,1);
Beta1(1,2,i-1) = B(2,1);
Beta1(2,2,i-1) = B(3,1);

%Quiver plots (for debugging!)
%
figure;
hold on;
%
plot(defXY1(x_pt_loc,1),defXY1(x_pt_loc,2),'ro')
%
plot(defXY1(i,1),defXY1(i,2),'bo')
%
plot(defXY1(y_pt_loc,1),defXY1(y_pt_loc,2),'go')
%
quiver(defXY1(x_pt_loc,1),defXY1(x_pt_loc,2),forceXY1(x_pt_loc,1)/50,forceXY1(x_pt_
loc,2)/50,'r')
%
quiver(defXY1(i,1),defXY1(i,2),forceXY1(i,1)/50,forceXY1(i,2)/50,'r')
%
quiver(defXY1(y_pt_loc,1),defXY1(y_pt_loc,2),forceXY1(y_pt_loc,1)/50,forceXY1(y_pt_
loc,2)/50,'r')

```

```

%
    quiver(defXY1(x_pt_loc,1),defXY1(x_pt_loc,2),Fxab/50,Fyab/50,'k')
%
    quiver(defXY1(y_pt_loc,1),defXY1(y_pt_loc,2),Fxbc/50,Fybc/50,'k')
%
    quiver(defXY1(i,1),defXY1(i,2),Xab,Yab,'g')
%
    quiver(defXY1(i,1),defXY1(i,2),Xbc,Ybc,'g')
    close all;

end
Bs1_filt = low_filt(30, 3, 1, Bs1)';
%save ellipsedata.mat Bs1_filt defXY1 forceXY1

%%
figure;
trails = [];
vidWriter = VideoWriter('Exo_test_stiffness_viz1.avi');
open(vidWriter);
for i = 1:100;%length(Bs1);
    K = [Bs1_filt(1,i) Bs1_filt(2,i); Bs1_filt(2,i) Bs1_filt(3,i)];
% K = [Bs1(1,i) Bs1(2,i); Bs1(2,i) Bs1(3,i)];
    [V(:,:,i) D(:,:,i)] = eig(K);
    if D(:,:,i) < 0
        continue
    end
    if i == 1
        trails = [defXY1(i,1),defXY1(i,2)];
        h5 = plot(trails(:,1), trails(:,2), '.', 'Color', [.8 .8 .8]);
        hold on
        h1 = plot(defXY1(i,1),defXY1(i,2),'ko', 'linewidth',2, 'markersize',8);
        h2 = quiver(defXY1(i,1),defXY1(i,2),forceXY1(i,1)/50,forceXY1(i,2)/50,'r',
        'linewidth',2);
        h3 = quiver(defXY1(i,1),defXY1(i,2),D(1,1,i)*V(1,1,i)/10,
        D(1,1,i)*V(2,1,i)/10,'k', 'linewidth',2);
        h4 = quiver(defXY1(i,1),defXY1(i,2),D(2,2,i)*V(1,2,i)/10,
        D(2,2,i)*V(2,2,i)/10,'k', 'linewidth',2);
        h6 = ellipse(sqrt((D(1,1,i)*V(1,1,i)/10)^2 +
        (D(1,1,i)*V(2,1,i)/10)^2),sqrt((D(2,2,i)*V(1,2,i)/10)^2 +
        (D(2,2,i)*V(2,2,i)/10)^2),atan((D(1,1,i)*V(2,1,i)/10)/
        (D(1,1,i)*V(1,1,i)/10)),defXY1(i,1),defXY1(i,2),'b',3000);
        pause
        axis([-12 4, -18 4]);

        %filename = strcat('C:\Users\Nic\Documents\MATLAB\Image
Processing\test1\frames\frame',num2str(i),'.png');
        %print('-dpng','-r300',filename);
        frame = getframe;
        %frame = imread(filename);
        writeVideo(vidWriter,frame);

    else
        set(h6, 'Visible','off');
        set(h5, 'XData', trails(:,1));
        set(h5, 'YData', trails(:,2));
        set(h1, 'XData', defXY1(i,1));
        set(h1, 'YData', defXY1(i,2));
        set(h2, 'XData', defXY1(i,1));
        set(h2, 'YData', defXY1(i,2));
        set(h3, 'XData', defXY1(i,1));
        set(h3, 'YData', defXY1(i,2));
        set(h4, 'XData', defXY1(i,1));
    end
end

```

```

set(h4, 'YData', defXY1(i,2));
set(h2, 'UData', forceXY1(i,1)/50);
set(h2, 'VData', forceXY1(i,2)/50);
set(h3, 'UData', D(1,1,i)*V(1,1,i)/10);
set(h3, 'VData', D(1,1,i)*V(2,1,i)/10);
set(h4, 'UData', D(2,2,i)*V(1,2,i)/10);
set(h4, 'VData', D(2,2,i)*V(2,2,i)/10);
h6 = ellipse(sqrt((D(1,1,i)*V(1,1,i)/10)^2 +
(D(1,1,i)*V(2,1,i)/10)^2),sqrt((D(2,2,i)*V(1,2,i)/10)^2 +
(D(2,2,i)*V(2,2,i)/10)^2),atan((D(1,1,i)*V(2,1,i)/10)/
(D(1,1,i)*V(1,1,i)/10)),defXY1(i,1),defXY1(i,2),'b',3000);
trails = [trails; defXY1(i,1),defXY1(i,2)];
drawnow;
%filename = strcat('C:\Users\Nic\Documents\MATLAB\Image
Processing\frame',num2str(i),'.png');
%print('-dpng','-r300',filename);
frame = getframe;
%frame = imread(filename);
writeVideo(vidWriter,frame);
pause(.01)

end
end

close(vidWriter);

%%
% Okay, now do the same thing for second test.

% Frame ~20 is first impulse (force sample 510)
% Frame ~1695 is second impulse (force sample 14508)
% 1675 frames, 13998 samples

% Snag relevant data between impulses.
defXY2(:,1) = test2Vid.deformationXandY(20:ds:1695,1);%*2.54; % make x deformation
positive
defXY2(:,2) = -test2Vid.deformationXandY(20:ds:1695,2);%*2.54;
angles2 = test2Vid.forceAngles(20:ds:1695)-180;
m = length(defXY2(:,1)) - 1;

forceMatrix2 = zeros(4,m-1);
defMatrix2 = zeros(4,3,m-1);
Beta2 = zeros(2,2,m-1);
Bs2 = zeros(3,m-1);

% Grab x and y components of force.
test2Data.force = test2Data.force - min(test2Data.force);
forceXY2(:,1) = -test2Data.force(1:ds:end).*cosd(angles2);
forceXY2(:,2) = test2Data.force(1:ds:end).*sind(angles2);

% Get stiffness matrix for each frame.

for i = 2:m

% (i-1) = point a
% i = point b
% (i+1) = point c

xdiff = abs(defXY2(:,1)-defXY2(i,1));

```

```

xdiff_inx = find(xdiff > .1);
[xmin xinx] = min(xdiff(xdiff_inx));% + .01*abs(i-[1:length(xdiff_inx)]'));
x_pt_loc = xdiff_inx(xinx);

ydiff = abs(defXY2(:,2)-defXY2(i,2));
ydiff_inx = find(ydiff > .5);
[ymin yinx] = min(ydiff(ydiff_inx));% + .01*abs(i-[1:length(ydiff_inx)]'));
y_pt_loc = ydiff_inx(yinx);

Fxab = forceXY2(x_pt_loc,1) - forceXY2(i,1); %
Fyab = forceXY2(x_pt_loc,2) - forceXY2(i,2); %
Fxbc = forceXY2(y_pt_loc,1) - forceXY2(i,1); %-
Fybc = forceXY2(y_pt_loc,2) - forceXY2(i,2); %-

% Populate force matrix with each vector.
Y = [Fxab; Fyab; Fxbc; Fybc];
forceMatrix2(:,i-1) = Y;

% Define quantities for displacement vector.
Xab = defXY2(x_pt_loc,1) - defXY2(i,1); %-
Yab = defXY2(x_pt_loc,2) - defXY2(i,2); %-
Xbc = defXY2(y_pt_loc,1) - defXY2(i,1); %+
Ybc = defXY2(y_pt_loc,2) - defXY2(i,2); %+

X = [Xab Yab 0;    % for each eqn., Fxab = Kxx(Xab) + Kth(Yab + Xab) + Kyy(Yab)
      0 Xab Yab;
      Xbc Ybc 0;
      0 Xbc Ybc];

% Populate matrix of deformation matrices (3D)
defMatrix2(:,:,:,i-1) = X;

% Populate Beta matrix with least-squares regression.
B = (X'*X)\(X'*Y); % MATLAB suggested I use this instead of inv(X'*X)*X'*Y
if abs(mean(B)) > 100 | sum(isnan(B)) > 0
    Bs2(:,i-1) = [0;0;0];
else
    Bs2(:,i-1) = B;
end

% Reshape Beta column into 2*2 (3D)
Beta2(1,1,i-1) = B(1,1);
Beta2(2,1,i-1) = B(2,1);
Beta2(1,2,i-1) = B(2,1);
Beta2(2,2,i-1) = B(3,1);

% Quiver plots (for debugging!)
% figure;
% hold on;
% plot(defXY2(x_pt_loc,1),defXY2(x_pt_loc,2),'ro')
% plot(defXY2(i,1),defXY2(i,2),'bo')
% plot(defXY2(y_pt_loc,1),defXY2(y_pt_loc,2),'go')
% %quiver(defXY2(i-1,1),defXY2(i-1,2),forceXY2(i-1,1)/50,forceXY2(i-1,2)/50,'r')
% %quiver(defXY2(i,1),defXY2(i,2),forceXY2(i,1)/50,forceXY2(i,2)/50,'r')
% %quiver(defXY2(i+1,1),defXY2(i+1,2),forceXY2(i+1,1)/50,forceXY2(i+1,2)/50,'r')
% quiver(defXY2(x_pt_loc,1),defXY2(x_pt_loc,2),Fxab/50,Fyab/50,'k')

```

```

%     quiver(defXY2(y_pt_loc,1),defXY2(y_pt_loc,2),Fxbc/50,Fybc/50,'k')
%     quiver(defXY2(i,1),defXY2(i,2),Xab,Yab,'g')
%     quiver(defXY2(i,1),defXY2(i,2),Xbc,Ybc,'g')
%     close all;

end
Bs2_filt = low_filt(30, 3, 1, Bs2)';
save ellipsedata2.mat Bs2_filt defXY2 forceXY2
%%
figure
trails = [];
for i = 1:length(Bs2);
    K = [Bs2_filt(1,i) Bs2_filt(2,i); Bs2_filt(2,i) Bs2_filt(3,i)];
    %K = [Bs2(1,i) Bs2(2,i); Bs2(2,i) Bs2(3,i)]; % Unfiltered
    [V(:,:,i) D(:,:,i)] = eig(K);
    if D(:,:,i) < 0
        continue
    end
    if i == 1
        trails = [defXY2(i,1),-defXY2(i,2)];
        h5 = plot(trails(:,1), trails(:,2), '.', 'Color', [.8 .8 .8]);
        hold on
        h1 = plot(defXY2(i,1),defXY2(i,2),'ko', 'linewidth',2, 'markersize',8);
        h2 = quiver(defXY2(i,1),defXY2(i,2),forceXY2(i,1)/50,forceXY2(i,2)/50,'r',
        'linewidth',2);
        h3 = quiver(defXY2(i,1),defXY2(i,2),D(1,1,i)*V(1,1,i)/10,
        D(1,1,i)*V(2,1,i)/10,'k', 'linewidth',2);
        h4 = quiver(defXY2(i,1),defXY2(i,2),D(2,2,i)*V(1,2,i)/10,
        D(2,2,i)*V(2,2,i)/10,'k', 'linewidth',2);
        trails = [defXY2(i,1),-defXY2(i,2)];
        axis([-16 16, -50 2]);
        axis('equal')
        pause
    else
        set(h5, 'XData', trails(:,1));
        set(h5, 'YData', trails(:,2));
        set(h1, 'XData', defXY2(i,1));
        set(h1, 'YData', defXY2(i,2));
        set(h2, 'XData', defXY2(i,1));
        set(h2, 'YData', defXY2(i,2));
        set(h3, 'XData', defXY2(i,1));
        set(h3, 'YData', defXY2(i,2));
        set(h4, 'XData', defXY2(i,1));
        set(h4, 'YData', defXY2(i,2));
        set(h2, 'UData', forceXY2(i,1)/25);
        set(h2, 'VData', forceXY2(i,2)/25);
        set(h3, 'UData', D(1,1,i)*V(1,1,i)/2);
        set(h3, 'VData', D(1,1,i)*V(2,1,i)/2);
        set(h4, 'UData', D(2,2,i)*V(1,2,i)/2);
        set(h4, 'VData', D(2,2,i)*V(2,2,i)/2);
        trails = [trails; defXY2(i,1),defXY2(i,2)];
        drawnow;xlabel('X deformation (cm)'); ylabel('Y deformation (cm)');
        title('Spring Stiffness Characterization');
        pause(.01)
    end
end

```

```

%%
% This section's mostly about plotting stuff.

% Relevant sections of force sensor data.
force1 = test1Data.force(1:ds:end);
force2 = test2Data.force(1:ds:end);
time1 = test1Data.time(1:ds:end);
time2 = test2Data.time(1:ds:end);

% Plot all the forces and deformations to see if positive lines up with
% positive and all that. Note: units are all different for everything.

figure; subplot(2,1,1);
[AX,H1,H2] = plotyy(time1,-forceXY1(:,2),time1,-defXY1(:,2)*2.54,'plot');
set(get(AX(1),'Ylabel'),'String','Force (N)')
set(get(AX(2),'Ylabel'),'String','Deformation (cm)'); hold on;
set(H1,'linewidth',2);
set(H2,'LineWidth',2);
title('Test 1 Results');
xlabel('Time (s)');
subplot(2,1,2);
[AX,H1,H2] = plotyy(time2,-forceXY2(:,2),time2,-defXY2(:,2)*2.54,'plot');
set(get(AX(1),'Ylabel'),'String','Force (N)')
set(get(AX(2),'Ylabel'),'String','Deformation (cm)'); hold on;
set(H1,'linewidth',2);
set(H2,'LineWidth',2);
title('Test 2 Results');
xlabel('Time (s)');
figure;
plot(time1,forceXY1(:,1),'k'); hold on; % X force
plot(time1,forceXY1(:,2),'b'); % Y force
plot(time1,defXY1(:,1),'r'); % X deformation
plot(time1,defXY1(:,2),'g'); % Y deformation
title('Test 1'); legend('X force','Y force','X def','Y def');
xlabel('Time (s)'); ylabel('Force (N)');
subplot(2,1,2);
plot(time2,forceXY2(:,1),'k'); hold on;
plot(time2,forceXY2(:,2),'b');
plot(time2,defXY2(:,1),'r');
plot(time2,defXY2(:,2),'g');
title('Test 1'); legend('X force','Y force','X def','Y def');
xlabel('Time (s)'); ylabel('Force (N)');

% Search for negative principle stiffnesses.
i1 = find(Beta1(1,1,:)<0 | Beta1(2,2,:)<0);

% Plot negative principle stiffness on force data.
figure; plot(time1,force1,'k.-'); hold on;
plot(time1(i1),force1(i1),'ro');
title('Test 1 negative principle stiffness locations');

% Search for negative principle stiffnesses.
i2 = find(Beta2(1,1,:)<0 | Beta2(2,2,:)<0);

% Plot negative principle stiffness on force data.
figure; plot(time2,force2,'k.-'); hold on;
plot(time2(i2),force2(i2),'ro');
title('Test 2 negative principle stiffness locations');

```